

A Conceptual Design of the Reactor Cavity Cooling System for the Horizontal Compact High Temperature Gas Reactor (HC-HTGR)

Nuclear Science and Engineering Division

About Argonne National Laboratory

Argonne is a U.S. Department of Energy laboratory managed by UChicago Argonne, LLC under contract DE-AC02-06CH11357. The Laboratory's main facility is outside Chicago, at 9700 South Cass Avenue, Lemont, Illinois 60439. For information about Argonne and its pioneering science and technology programs, see www.anl.gov.

DOCUMENT AVAILABILITY

Online Access: U.S. Department of Energy (DOE) reports produced after 1991 and a growing number of pre-1991 documents are available free at OSTI.GOV (<http://www.osti.gov/>), a service of the US Dept. of Energy's Office of Scientific and Technical Information.

Reports not in digital format may be purchased by the public from the National Technical Information Service (NTIS):

U.S. Department of Commerce
National Technical Information Service
5301 Shawnee Rd
Alexandria, VA 22312
www.ntis.gov
Phone: (800) 553-NTIS (6847) or (703) 605-6000
Fax: (703) 605-6900
Email: orders@ntis.gov

Reports not in digital format are available to DOE and DOE contractors from the Office of Scientific and Technical Information (OSTI):

U.S. Department of Energy
Office of Scientific and Technical Information
P.O. Box 62
Oak Ridge, TN 37831-0062
www.osti.gov
Phone: (865) 576-8401
Fax: (865) 576-5728
Email: reports@osti.gov

Disclaimer

This report was prepared as an account of work sponsored by an agency of the United States Government. Neither the United States Government nor any agency thereof, nor UChicago Argonne, LLC, nor any of their employees or officers, makes any warranty, express or implied, or assumes any legal liability or responsibility for the accuracy, completeness, or usefulness of any information, apparatus, product, or process disclosed, or represents that its use would not infringe privately owned rights. Reference herein to any specific commercial product, process, or service by trade name, trademark, manufacturer, or otherwise, does not necessarily constitute or imply its endorsement, recommendation, or favoring by the United States Government or any agency thereof. The views and opinions of document authors expressed herein do not necessarily state or reflect those of the United States Government or any agency thereof, Argonne National Laboratory, or UChicago Argonne, LLC.

A Conceptual Design of the Reactor Cavity Cooling System for the Horizontal Compact High Temperature Gas Reactor (HC-HTGR)

prepared by
Yeongshin Jeong, Darius Lisowski, Qiuping Lv, and Rui Hu
Nuclear Science and Engineering Division, Argonne National Laboratory

September 2023

ABSTRACT

Horizontal Compact High Temperature Gas Reactor (HC-HTGR) is being designed by a multi-disciplinary team of nuclear, mechanical, and structural engineers under the support of a DOE-NE Advanced Reactor Demonstration Program's Advanced Reactor Concepts-20 (ARC-20) award. The objective of this ARC-20 project is to deliver a conceptual design for the proposed HC-HTGR in 3 years and support its commercialization as a safe, low-cost HTGR. Argonne National Laboratory (Argonne) is responsible for the design and analysis of the reactor cavity cooling system (RCCS) as a safety system for passive decay heat removal of the reactor concept.

This report documents the design study to derive a conceptual design study of the RCCS for the HC-HTGR. It includes the identification of the functions and requirements of the HC-HTGR RCCS, design analyses including high-level design consideration and the calculations for optimizing design space of the system with supporting component-level analysis to inform the material selection and performance of the water panel, the description of the conceptual design of the HC-HTGR RCCS derived based on the analyses results, and performance evaluation of the conceptual RCCS for the HC-HTGR.

A detailed concept of the RCCS has been identified and high-level system requirements has been developed for the HC-HTGR. Design space focusing on the natural circulation loop portion of the RCCS has been investigated to optimize the system performance. The initial baseline dimensions were firstly derived based on the scoping calculations. A component level design analysis was conducted for the water panel to inform the material selection and to assess its conduction performance. A preliminary system-level performance analysis was performed for the 1/8th of the compartment of the initial baseline design of the RCCS using RELAP5-3D. To improve the system thermal performance, the RCCS design has been updated by exploring various design options by design parametric analyses. Based on the results, the conceptual design of the RCCS for the HC-HTGR has been derived, which satisfies the target performance of $\sim 1 \text{ MW}_t$ at the elevated vessel wall temperature conditions.

Transient simulations were conducted for the conceptual RCCS design for the HC-HTGR under various operation modes and heat load conditions using RELAP5-3D. The system dynamics in different operating states was investigated and the system performance under transients of interest was evaluated. The results demonstrated the overall system feasibility that the RCCS design maintains structures temperatures lower than maximum allowable temperature with sufficient system inventory without any active heat removal in the design process with certain transients addressed. The HC-HTGR RCCS will have additional design updates of subsystems or optimization of the system components during the preliminary and final design phases. Since the entire plant has not been integrated yet, this delivered conceptual design is subject to changes for integration, that require additional conceptual design activities and Quality and Assurance implementation (Q&A). The performance assessment of the RCCS for the HC-HTGR will be then revisited and optimized to finalize the system design, and the RCCS integrated primary system analysis will be utilized to simulate selective accident scenarios of interest where efforts are currently undergoing in the project.

Table of Contents

ABSTRACT.....	I
TABLE OF CONTENTS	II
LIST OF FIGURES	III
LIST OF TABLES	IV
1 INTRODUCTION	1
2 FUNCTIONS AND REQUIREMENTS OF THE HC-HTGR RCCS	2
2.1 RCCS FUNCTIONS	2
2.2 DESIGN REQUIREMENTS OF THE RCCS.....	3
2.2.1 <i>Mechanical Requirements</i>	3
2.2.2 <i>Performance Requirements</i>	5
3 DESIGN ANALYSES OF THE HC-HTGR RCCS.....	6
3.1 DESIGN CONSIDERATIONS OF THE HC-HTGR RCCS	6
3.1.1 <i>System inventory</i>	6
3.1.2 <i>HVAC capacity</i>	7
3.2 DESIGN PROCESS OF THE HC-HTGR RCCS	9
3.2.1 <i>Scoping calculations</i>	9
3.2.2 <i>Water panel material study</i>	13
3.2.3 <i>Development of the water panel modeling approach</i>	17
3.2.4 <i>Preliminary performance analysis of the HC-HTGR RCCS</i>	23
3.2.5 <i>Design parametric study of the HC-HTGR RCCS</i>	25
4 A CONCEPTUAL DESIGN OF THE HC-HTGR RCCS	32
4.1 DESIGN DESCRIPTIONS.....	32
4.2 KEY SYSTEM COMPONENTS	33
4.3 OPERATING CONDITIONS	35
5 PERFORMANCE EVALUATION OF THE HC-HTGR RCCS.....	36
5.1 SYSTEM-LEVEL PERFORMANCE OF THE HC-HTGR RCCS	36
5.1.1 <i>RELAP5-3D model of the HC-HTGR RCCS</i>	36
5.1.2 <i>System performance by operating mode</i>	37
5.1.3 <i>System performance under various heat load conditions</i>	40
6 SUMMARY AND FUTURE WORK.....	48
REFERENCES	49
ACKNOWLEDGEMENT.....	50

LIST OF FIGURES

Figure 1 Reactor room dimensions of the pre-conceptual HC-HTGR in 2021-2022 (provided by Boston Atomics).....	4
Figure 2 Initial design of the vertical supports of the HC-HTGR (provided by Boston Atomics) [1].....	5
Figure 3 Reference decay power rates used to estimate the system inventory [6,7].....	6
Figure 4 Schematics of anticipated internal air circulation in the HC-HTGR reactor cavity	8
Figure 5 Estimated heat transfer through internal air circulation and temperature rise of the air	8
Figure 6 A flowchart of the standalone RCCS analysis	9
Figure 7 Thermal resistance network of the water panel design	10
Figure 8 A schematic of a representative natural circulation loop of the HC-HTGR RCCS.....	10
Figure 9 Standalone RCCS analysis results – $T_{RPV}=472\text{ }^{\circ}\text{C}$, $T_{\text{water}}=60\text{ }^{\circ}\text{C}$	11
Figure 10 Isometric view of the baseline design of RCCS for HC-HTGR (Not scaled)	12
Figure 11 CFD domain of the test case	13
Figure 12 Comparison of the water panel temperature by pipe materials ($T_{RPV}=220\text{ }^{\circ}\text{C}$ condition).....	14
Figure 13 Comparison of the water panel temperature by pipe materials ($T_{RPV}=472\text{ }^{\circ}\text{C}$ condition).....	14
Figure 14 Comparison of heat flow by pipe material in constant temperature boundary conditions	15
Figure 15 Fouling resistance versus change in flow velocity, based on correlation from [13]	16
Figure 16 Reduction in heat transfer coefficient assuming log and power trends vs time.....	16
Figure 17 Schematics of RELAP5-3D modeling approaches of the water panel	18
Figure 18 RELAP5-3D nodalization diagram of the test case by the modeling approach.....	20
Figure 19 Nodalization diagram of the RELAP5-3D model for the pre-conceptual RCCS design [17]	23
Figure 20 Major design changes of the water panel of HC-HTGR RCCS (Not scaled).....	25
Figure 21 The RPV temperature and natural circulation flow rate during DCC (natural circulation flow rate after boiling mass flow rate was omitted.).....	28
Figure 22 Potential design updates of the vertical supports for the HC-HTGR (as of Dec. 2022, provided by Boston Atomics.).....	28
Figure 23 Updated design parametric study results	30
Figure 24 A schematic of the water panel and tank design of the conceptual HC-HTGR RCCS	31
Figure 25 A system configuration of the conceptual design of the HC-HTGR RCCS	32
Figure 26 Dimensions of the conceptual design of the HC-HTGR RCCS (not scaled, single loop).....	33
Figure 27 Connection between the upper plenum and the riser tubes.....	34
Figure 28 Nodalization diagram of the RELAP5-3D model used in design calculations.....	37

Figure 29 Comparison of the water panel temperature at the design condition by operation mode	38
Figure 30 Temperature distribution of the water panel at the design condition by operation mode	39
Figure 31 Heat load to RCCS during DCC (Scaled from Framatome's input) [17].....	41
Figure 32 Transient behavior of RCCS for the HC-HTGR under the hypothetical DCC heat load	42
Figure 33 RCCS performance under the hypothetical DCC heat load.....	43
Figure 34 Heat load to RCCS bounding case provided by Boston Atomics – vessel average heat flux	44
Figure 35 Transient behavior of RCCS for the HC-HTGR under heat load provided by Boston Atomics	45
Figure 36 RCCS performance under heat load provided by Boston Atomics	46
Figure 37 Comparison of various heat loads on RCCS with long term decay heat of HC-HTGR	47

LIST OF TABLES

Table 1 High-level design requirements applicable to the HC-HTGR RCCS	3
Table 2 Single water panel conduction performance test matrix	13
Table 3 Dimensions of the RELAP5 test case.....	19
Table 4 Specifications of the panel and the pipe heat structure inputs by the modeling approach	21
Table 5 Comparison of the test case results of RELAP5-3D and CFD - $T_{RPV}=220\text{ }^{\circ}\text{C}$	22
Table 6 Comparison of the test case results of RELAP5-3D and CFD - $T_{RPV}=472\text{ }^{\circ}\text{C}$	22
Table 7 Performance of 1/8 th compartment of the pre-conceptual RCCS design.....	24
Table 8 Comparison of the water panel design performance	26
Table 9 Thermal performance by top tank injection elevation (X) and top tank elevation (Y) in the design condition.....	27
Table 10 Updated design parametric test matrix for the water panel.....	29
Table 11 Performance the updated RCCS design	31
Table 12 Specifications of the water panel of the conceptual HC-HTGR RCCS design.....	33
Table 13 Performance of the RCCS at the design condition by operation mode.....	39

1 Introduction

The Horizontal Compact High Temperature Gas Reactor (HC-HTGR) is being designed by a multi-disciplinary team of nuclear, mechanical, and structural engineers led by MIT under the support of a DOE-NE Advanced Reactor Demonstration Program's Advanced Reactor Concepts-20 (ARC-20) award. The objective of this ARC-20 project is to deliver a conceptual design for the proposed HC-HTGR in 3 years and support its commercialization as a safe and low-cost HTGR with a focus on minimizing the overnight capital cost of the power-generation system and explicit considerations of functionality, constructability, transportability, modularity, safety, and future licensing.

The HC-HTGR concept is a prismatic high-temperature gas-cooled reactor in a horizontal layout with a total power of 160-230 MW_t. The HC-HTGR integrates the reactor pressure vessel (RPV) and steam generator into a single vessel. It has a horizontal orientation to achieve its construction cheaper and faster, instead of a vertical alignment of traditional HTGR and steam generator housed in the tall reactor building [1]. This poses additional challenges for passive decay heat removal using the reactor cavity cooling system (RCCS) concept, which uses natural forces to provide safe and dependable ex-vessel cooling during emergencies by natural circulation.

Argonne National Laboratory ("Argonne") is responsible for the design and analysis of the reactor cavity cooling system (RCCS) as a safety system for passive decay heat removal of the reactor concept. The pre-conceptual design of the HC-HTGR RCCS was a system of two tanks above and below the RPV connected by pipes and a natural circulation-driven water panel design similar to traditional RCCS such as next generation nuclear plant (NGNP) [2]. This report documents the design work to derive the conceptual design of the HC-HTGR RCCS performed for FY22-FY23. It includes functions and requirements, a system description, and performance of the HC-HTGR RCCS design.

Functional and design requirements of the RCCS for the HC-HTGR were established first to guide design activities and initial scoping calculations, which includes a high-level design calculation to determine the water inventory, estimate a heating, ventilation, and air-conditioning (HVAC) thermal capacity, and design scoping calculations. This work is detailed in Chapter 2.

Design analyses were performed to develop the detailed concept of the RCCS for the HC-HTGR by scoping calculations to narrow down the design space, a component-level analysis to inform material selection and the conduction performance for the water panel, preliminary performance analysis for the initial baseline dimensions of the system, and design parametric analysis for updating system design to improve the thermal performance. This work is detailed in Chapter 3.

The conceptual design of the HC-HTGR RCCS has been derived based on the design parametric analyses. Descriptions of the RCCS design, system configurations, key components, and operating conditions of the RCCS are described in Chapter 4.

To demonstrate overall system feasibility of the HC-HTGR RCCS, a system-level analysis was conducted using RELAP5-3D by operation mode and various heat load conditions to investigate the system dynamics under anticipated RCCS operating regimes, beginning with single-phase natural circulation, progressing to two-phase natural circulation, and gradual boil-off of the coolant inventory. This work is detailed in Chapter 5.

2 Functions and Requirements of the HC-HTGR RCCS

The RCCS is a safety-related system that provides a passive means of removing decay heat in the core when the power conversion system, the primary and secondary heat transport systems, and the normal shutdown cooling system are unavailable to remove decay heat [3]. As a means for ex-vessel cooling, the RCCS achieves heat removal by radiation and convection cooling from the reactor pressure vessel walls to a network of cooling channels. The RCCS is designed to use natural forces and be relatively simple and the potential for high levels of passive safety performance via removal of core decay heat during off-normal conditions. There are design variations that have been chosen to feature specific reactor types and design choices such as primary coolant, geometry, and dimensions of individual cooling channels, for instance, General Atomics (GA) modular high temperature gas-cooled reactor (MHTGR) [4], Next Generation Nuclear Plant (NGNP) [2], and Framatome Steam Cycle – High Temperature Gas Cooled Reactor (SC-HTGR) [5].

Since the concept of the HC-HTGR is characterized horizontal and modules in-line with one another in relatively small reactor building [1], it brought challenges in developing an RCCS design that targeted a high level of performance of ex-vessel natural circulation with relative simplicity and inherent safety characteristics with reduced system volume and height. GA's MHTGR and NGNP are good references for the basis of system design requirements, where both have undergone the license application process in the past. Since they adopted the air-cooled natural convection open loop type system, those requirements could be modified to be applicable to other concepts of the RCCS, such as the water-based design or the design having different operating strategies. Based on those, a set of functional and performance requirements have been established for the HC-HTGR RCCS design. These requirements have been prepared to provide a guidance for preliminary design envelopes and the initial performance assessment.

2.1 RCCS functions

The key functional requirements of the RCCS are defined with an acceptable RPV wall temperature and a reactor cavity concrete temperature during power operation, startup, shutdown, anticipated operational occurrences (AOOs), and various Design Basis Events (DBEs). Working with the project team, design requirements applicable to the HC-HTGR RCCS have been derived in Table 1, where its design-specific values and features are represented in bold. It can be modified in response to advancements in the core and nuclear system design, as well as in the plant configurations of the HC-HTGR. Additional design requirement categories, such as codes and standards, physical protection, material control, and safeguards, quality assurance, construction, or decommissioning requirements were considered but have not been included in the table.

Table 1 High-level design requirements applicable to the HC-HTGR RCCS

Category	Descriptions
System configuration and essential features requirements	<p>1.1) The RCCS shall remove heat from the reactor cavity by passive means.</p> <p>1.2) The RCCS heat transfer surfaces shall remove heat from the full length and circumference of the reactor vessel.</p> <p>1.3) The RCCS shall accommodate reactor vessel vertical supports, axial supports, and perhaps shutdown circulator openings and lateral restraint structure</p>
Operational requirements	<p>1.4) If required based on containment design and function, the RCCS shall maintain reactor cavity concrete temperatures less than 65 °C during normal operation and less than 177 °C for off-normal events.</p> <p>1.5) The heat loss through the RCCS will be as low as reasonably achievable while the reactor is operating between 0 % and 100 % power. A target maximum heat loss is ~1 MW_t.</p> <p>1.6) The RCCS shall limit the maximum reactor vessel temperature below 427 °C for a pressurized conduction cooldown and below 482 °C for a depressurized conduction cooldown</p> <p>1.7) As designed for continuous operation, the RCCS heat load during normal plant operation will be based on the normal operating conditions.</p> <p>1.8) The RCCS will be designed for an operating life of 40 years.</p>
Structural requirements	<p>1.9) All components and piping of the RCCS shall be designed against seismic loads and tornado.</p>

2.2 Design requirements of the RCCS

2.2.1 Mechanical Requirements

The mechanical design of the RCCS could be constrained by the physical dimensions and relative positions of the reactor building, the reactor pressure vessel, and the reactor core. Key constraints were mainly established by the radial and axial dimensions of the reactor building and the RPV for the pre-conceptual design of the RCCS. Figure 1 shows the reactor building dimensions including positions of the RPV and space of the RCCS for the HC-HTGR provided by Boston Atomics. The reactor room dimensions: 9.2 m of the width and 7.9 m of the height constrains the RCCS design space, targeting total reactor building height of 10.4 m to make it compact at the best extent. The RPV has 4.1 m of outer diameter and 12 m of the total length with 10 m of the core length. Therefore, the size of the tank could be limited by the space, where it has 3.1 m and 0.7 m between the RPV top and the ceil, and low and the basement respectively. Since the nature of the design is iterative, the dimensions and constrains have been somewhat modified through the process, and it is likely that will still be somewhat modified in the future, within bounds were feasibility, safety and constructability are kept.

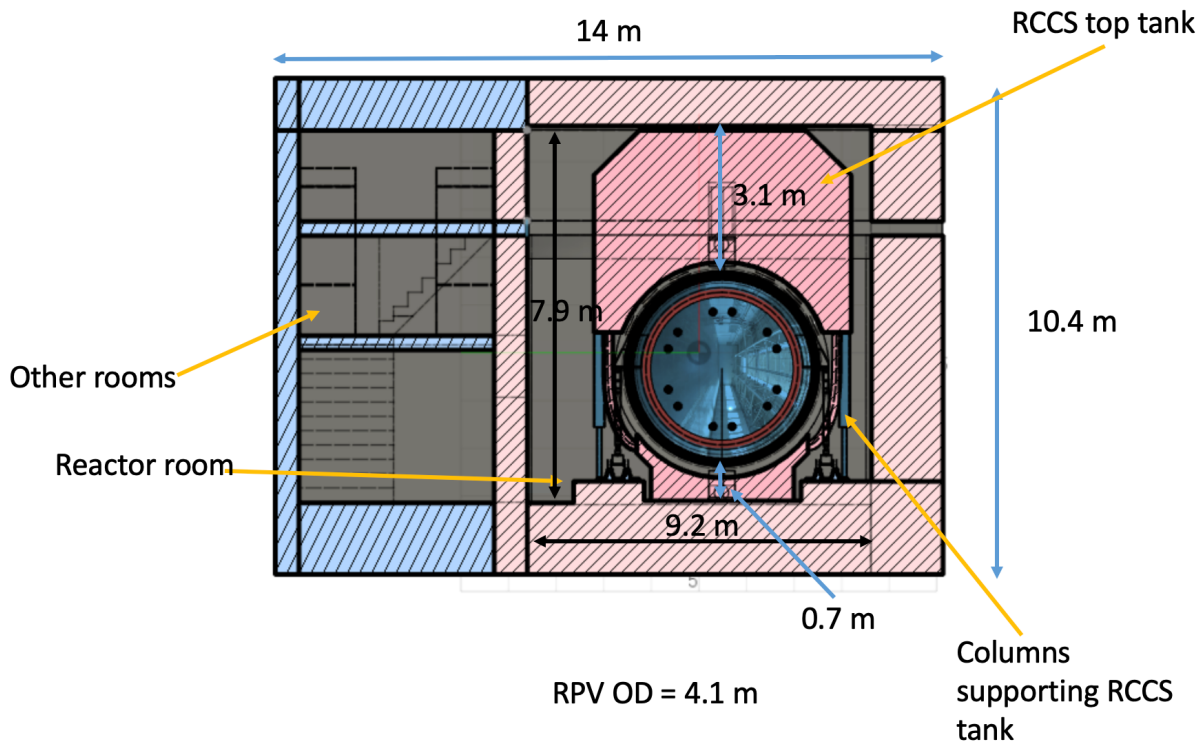
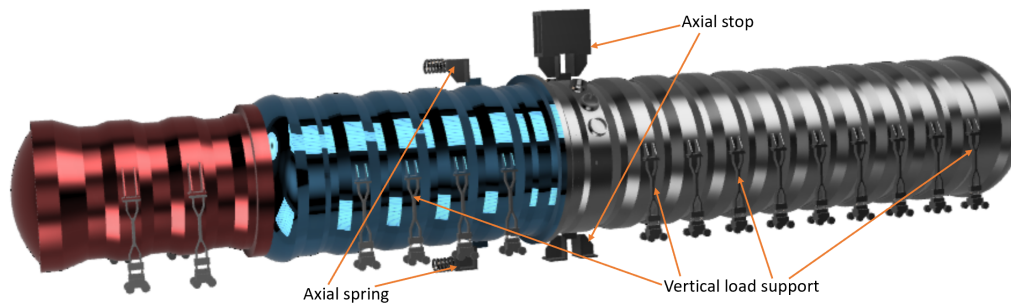


Figure 1 Reactor room dimensions of the pre-conceptual HC-HTGR in 2021-2022 (provided by Boston Atomics)

Figure 2 shows the structural supports of the RPV and the primary system of the HC-HTGR, which would establish mechanical interface with the RCCS. There are two main groups of structural supports: the vertical load supports and the axial supports. In 2021-2022, the pre-conceptual design of the HC-HTGR had 8 vertical load supports on each side of the RPV equally spaced, 1.5 m in the axial direction. It limits a width of a single water panel as it is located between each vertical support, but the actual allowable width might be constrained lower than that as the specific dimensions of the vertical supports have not been finalized. It should be noted here that this was the pre-conceptual design of the structural supports of the RPV, and it has been potentially updated after design iterations with the project team based on the design analysis results, which will be described in Section 3.2.5.



* Used under the terms of the CC BY license (<https://creativecommons.org/licenses/by/4.0/>)
Figure 2 Initial design of the vertical supports of the HC-HTGR (provided by Boston Atomics)
[1]

2.2.2 Performance Requirements

A set of performance requirements has been established for the HC-HTGR RCCS. These are prepared to be sufficient to guide preliminary design activities and scoping performance calculations, although in the future may change once integrating with the rest of the plant design. These performance requirements and design objectives are summarized as follows:

- The RCCS shall provide sufficient passive RPV cooling during accidents.
- The RCCS shall operate continuously during normal operation and off-normal conditions.
- The RCCS cooling loop shall rely on natural circulation for normal operation and accidents.
- The RCCS shall have multiple redundant independent loops.
- The RCCS shall accommodate the reactor building and reactor pressure vessel interfaces.
- The heat sink of the top water tank shall include actively cooled means during normal operation.
- Any active system to cool the system shall be assumed to be unavailable during accidents.
- The RCCS water tanks shall include replenishment either before or after the depletion of the initial inventory of water.
- (*Design objective*) The target heat removal rate of the RCCS shall be ~1 MWt without exceeding the allowable reactor pressure vessel temperature.
- (*Design objective*) The RCCS water tanks should contain sufficient inventory to sustain accident cooling for a period of greater than 7 days.

3 Design Analyses of the HC-HTGR RCCS

3.1 Design considerations of the HC-HTGR RCCS

The HC-HTGR RCCS design targets the reactor with a total power of 160 MW_t at first, such that it could be utilized for assessing the feasibility of the concept. An initial design process for the HC-HTGR RCCS included a determination of the total water inventory, an estimation of the HVAC capability, and scoping calculations to narrow down RCCS design space focusing on the natural circulation loop.

3.1.1 System inventory

According to the design objectives of the HC-HTGR RCCS, the total water inventory in the system should be sufficient to secure at least 7 days until the boil-off of all coolant inventory in the system. To estimate the total water inventory required, two reference decay heat data were considered: ANS standard [6] and calculation results from a reference HTGR [7], shown as the ratio of decay power (P) to the nominal power (P₀) in Figure 3. ANS standard is specific to light water reactors, in particular UO₂ fuel decay power curve. Afterheat power was calculated for GA's MHTGR modeled as a semi-homogeneous graphite-moderated core using a thorium-uranium cycle, where predicted results were slightly higher than that of ANS standard as a larger amount of thorium and ²³⁵U enrichment of the HTGR fuel considered in calculations [7].

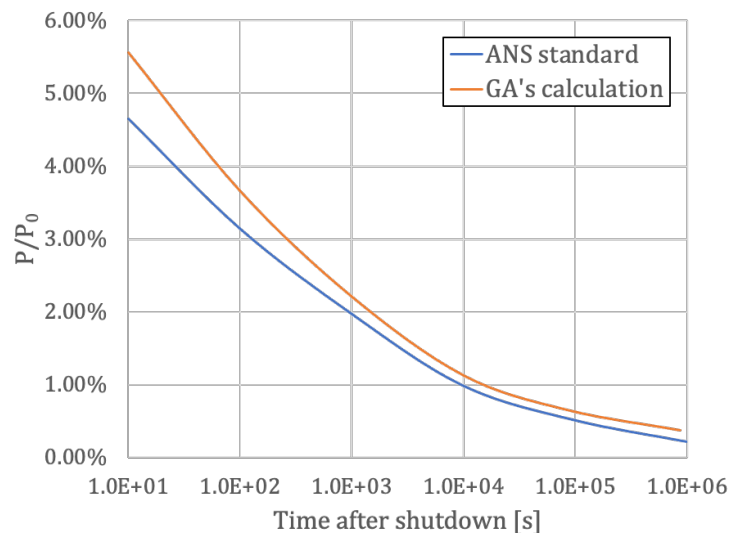


Figure 3 Reference decay power rates used to estimate the system inventory [6,7]

Assuming the RCCS is an open system operating in 1 atm and all decay heat is transferred to the RCCS coolant without any cooling that would otherwise be available during normal operation, the estimated amount of water required for securing 7 days of operation was approximately 170 tons and 220 tons of water for 160 MW_t HC-HTGR RCCS from the ANS standard and GA's decay heat curve, respectively. When the top tank is assumed to be mounted with its bottom above the top of the RPV having its height of 3.1 m and holds most of the water inventory of the system

about 200 tons, a single water tank has designed to 5.4 m of width, 3.1 m of height, and 12 m of the length. It could be adjusted by system configurations and optimized to accomplish design objectives in desired operation conditions of the HC-HTGR.

3.1.2 HVAC capacity

A potential strategy for cooling the reactor cavity of the HC-HTGR could be supported by heating, ventilating, and air conditioning (HVAC) systems along with the RCCS, whose capability might be adjustable to satisfy the design limits of the reactor building concrete and the RPV. In most cases, the RCCS is the only safety-related cooling system for the design, and the design of the HC-HTGR RCCS shall target potential licensing basis events to remove most of the decay heat from the core to protect the RPV and the reactor cavity concrete from overheating, together with the conduction through the reactor cavity concrete wall without HVAC when the reactor is shutdown. From the reactor building configuration of the HC-HTGR, a potential air flow is expected through the gap between adjacent panels, where the air between the RPV and the gap flows upward as heated and exits to the reactor cavity space. This feature might affect the reactor cavity concrete temperature as hot air directly contacts the concrete wall. Therefore, it is important to consider HVAC cooling as part of the RCCS design work to ensure the concrete temperature low enough during normal operating conditions of the HC-HTGR. To estimate the required HVAC cooling capability, lumped parameter analysis was performed considering anticipated internal air circulation in the reactor building.

Figure 4 shows a schematic of the anticipated internal air flow in the reactor building of the HC-HTGR considering the pre-conceptual layout of the RCCS design. The amount of the heat transfer from the RPV to the air was estimated by the gap flow rate and temperature difference of inflow and outflow air through the gap, and this can be estimated with the natural convective heat transfer coefficient (h) and gap air temperature as equation (1). Natural convective heat transfer coefficient was then obtained by the Churchill-Chu correlation for the external flow on a long horizontal cylinder as equation (2) [8], where T_{RPV} is the RPV surface temperature, T_{gap} is the air temperature at the gap, and D is the RPV diameter, respectively. In the analysis, assumptions were made for modeling simplicity that the natural convective heat transfer of the gap air with the panel surface was neglected, the ambient air temperature in the reactor building (T_{amb}) was considered as the inlet temperature of the gap air flow, and all of the heat transferred through the air flow was assumed transferred to the HVAC.

$$Q_{RPV \rightarrow air} = \dot{m}_{gap} C_p (T_{out} - T_{in}) = hA(T_{RPV} - T_{gap}), \text{ where } T_{in} = T_{amb} \quad (1)$$

$$Nu = \left[0.60 + \frac{0.387 Ra_D^{1/6}}{\left\{ 1 + \left(\frac{0.559}{Pr} \right)^{9/16} \right\}^{8/27}} \right]^2, \text{ where } Ra_D = \frac{g\beta(T_{RPV} - T_{gap})D^3}{\nu\alpha} \quad (2)$$

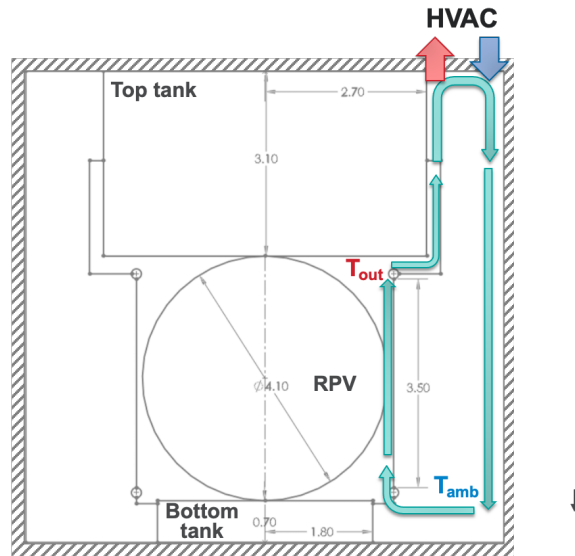


Figure 4 Schematics of anticipated internal air circulation in the HC-HTGR reactor cavity

The estimated heat transfer amount from the RPV and the air temperature rise through the gap by the ambient air temperature are shown in Figure 5. The estimated heat transfer amount was ~ 28 kW for the air temperature of 30°C and ~ 19 kW for the air temperature of 70°C , respectively. This can be covered by a generic HVAC, implying the reactor cavity concrete temperature can be controlled by maintaining the reactor building air temperature sufficiently low by HVAC during the normal operating conditions. The results also confirm that the RCCS is the major contributor of parasitic heat loss from the RPV during normal operation condition. Air temperature is increased via heat from the water panel from $\sim 4.9^\circ\text{C}$ to 6.2°C by the ambient temperature controlled by the HVAC. As air temperature rise is relatively low, the local influence of the air outlet temperature on the concrete wall is expected insignificant under the condition of the air ambient temperature being well-controlled by HVAC. It should be noted that it might require thermal shields for local regions potentially receiving direct thermal radiation from the reactor vessel wall.

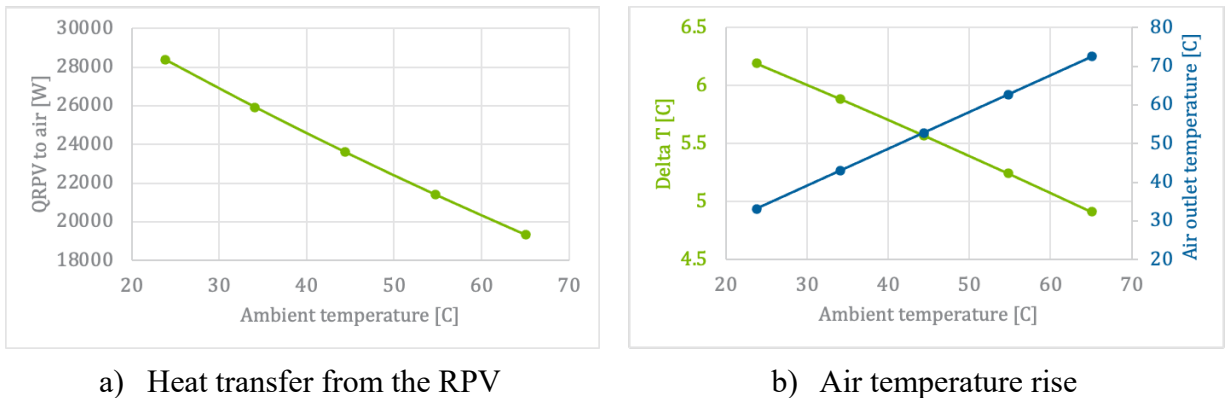


Figure 5 Estimated heat transfer through internal air circulation and temperature rise of the air

Since the amount of heat transfer by the internal air flow is small, RCCS is then the major contributor to the parasitic heat loss from the RPV in normal operational conditions. Nevertheless, air temperature variation in flowing direction might affect the panel temperature distribution, which was derived from previous experiences on Natural Convection Shutdown heat removal Test facility (NSTF), a scaled facility for the RCCS concept, on modeling the facility for predicting a heated plate temperature profile [9]. Therefore, it might require thermal shield for local regions, for instance at locations receiving the direct thermal radiation from the reactor vessel wall, even though HVAC is capable of controlling the internal building air temperature.

3.2 Design Process of the HC-HTGR RCCS

3.2.1 Scoping calculations

To narrow down a design space of a natural circulation loop for the HC-HTGR RCCS, a standalone RCCS analysis methodology has been established, which consists of a coupled thermal resistance network analysis and a simplified natural circulation loop analysis. Thermal resistance network analysis estimates the amount of heat transfer from the RPV in desirable RCCS operation conditions. The simplified natural circulation loop analysis predicts a natural circulation flow rate according to the system dimensions. Two steps are combined by exchanging the amount of coolant temperature increase across the riser tube (ΔT) and the natural convective heat transfer coefficient (h_{tc}) of the riser tube while iterating until achieving heat balance. With given conditions of the RPV temperature and coolant inlet temperature, the standalone RCCS analyses estimate natural circulation flow rate and heat removal rate by design parameters. The flowchart of the analysis is summarized in Figure 6.

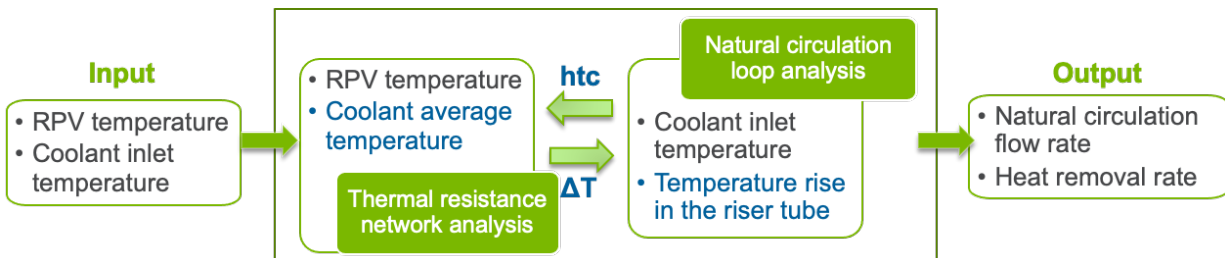


Figure 6 A flowchart of the standalone RCCS analysis

The domain of the thermal resistance network consists of the RPV, the panel, and the coolant in the riser tubes. Heat transfer in the gap from the uninsulated outer wall of the RPV to the RCCS riser tubes/panels consists of natural convection and thermal radiation. The convective and radiative components were assumed to be independent processes here. Natural convection was assumed for the RCCS heat transfer from the panel to the coolant in the riser tube. From the initial concept of the HC-HTGR RCCS, the panel was taken into account as a heat transfer fin. By assuming a sufficiently high efficiency of heat transfer between the panel and the riser tube, conductive heat transfer between the panel and the riser tube wall was ignored. A schematic of the representative thermal resistance network is shown in Figure 7.

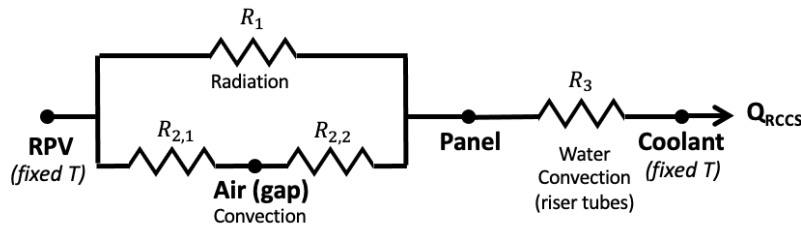


Figure 7 Thermal resistance network of the water panel design

The domain of the natural circulation loop analysis consists of the top/bottom tanks, the collectors, pipes connecting the tank and collector, riser tubes, and downcomer lines for half of the pre-conceptual design of RCCS for the HC-HTGR, as shown in Figure 8. For modeling simplicity, assumptions were made that fluid flow was a single-phase in a steady state, heat conduction from the panel to the fluid and inside the fluid was neglected, and a minimum number of elbows were considered in the form loss pressure drop calculation. Once a set of system dimensions and operation conditions which satisfy design requirements were sufficient to establish a natural circulation flow, the flow rate and the temperature difference between the hot and cold regions were calculated. The governing equation is derived from total pressure drop (ΔP_{total}) across the loop expressed in Equation (3), which consists of the sum of pressure drop from friction (ΔP_f), form loss (ΔP_{form}), acceleration (ΔP_{ac}), and head loss (ΔP_g) between two nodes divided into the inlet and outlet of each component.

$$\Delta P_{total} = \sum (\Delta P_{f,i} + \Delta P_{ac,i} + \Delta P_{g,i} + \Delta P_{form,i}) = 0$$

$$, \text{ where } \Delta P_f = f \frac{\sum L \rho v^2}{D_h} \frac{1}{2}, \Delta P_g = \rho g \Delta H, \Delta P_{ac} = \dot{m}^2 \left(\frac{1}{\rho_i} - \frac{1}{\rho_o} \right), \Delta P_{form} = \sum K_j \frac{\rho v^2}{2} \quad (3)$$

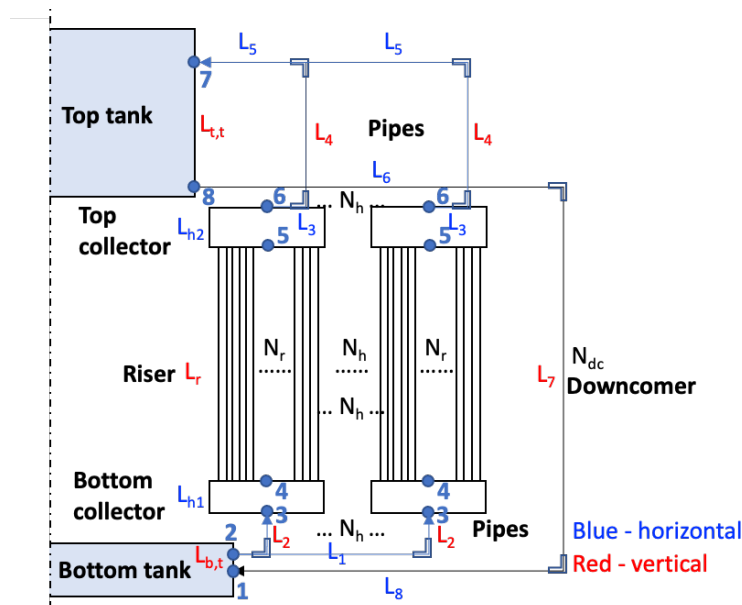


Figure 8 A schematic of a representative natural circulation loop of the HC-HTGR RCCS

Standalone RCCS analyses were performed using combinations of the RPV surface temperature from 220 °C to 472 °C and coolant bulk temperature from 30 °C to 70 °C, which ranges were expected to have during RCCS operating conditions. The natural circulation loop design space was considered to include 9 design parameters including the length of the cold leg, hot leg, and riser tube, the diameter of the collector, riser tube, and downcomer, the elevation difference between the inlet and outlet ports of the top tank and the bottom tank, and the pitch-to-diameter (P/D) ratio of the riser tubes assembly.

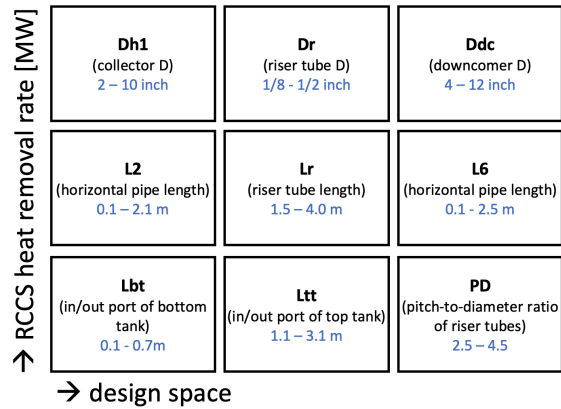


Figure 9 Standalone RCCS analysis results – $T_{RPV}=472\text{ }^{\circ}\text{C}$, $T_{water}=60\text{ }^{\circ}\text{C}$

For each case of the RPV temperature and water temperature conditions, a total ~262,000 (4 points per 9 design parameters) set of dimensions was explored to narrow down the design space range to have better performance in terms of the heat removal rate of RCCS. The results of the example case of the RPV and water temperature conditions are shown in Figure 9. The overall process narrowing down the design space was aimed toward maximizing heated length (riser tube length) and water panel surface area and making overall loop dimensions as compact as possible. The results helped to understand the influence of each design parameter of the RCCS for the HC-HTGR to the natural circulation performance and led to derive an initial set of the dimensions of the natural circulation loop of the RCCS. Based on the results, the baseline dimensions of the HC-HTGR RCCS were firstly derived as shown Figure 10. It should be noted that some of the design parameters were determined based on engineering judgment by consulting the project team. For instance, the elevation change of the inlet and outlet ports of the bottom tanks is set as 0.65 m to secure marginal space for engineering purposes, while a smaller value is preferable showing this change had a minimal influence on the RCCS performance.

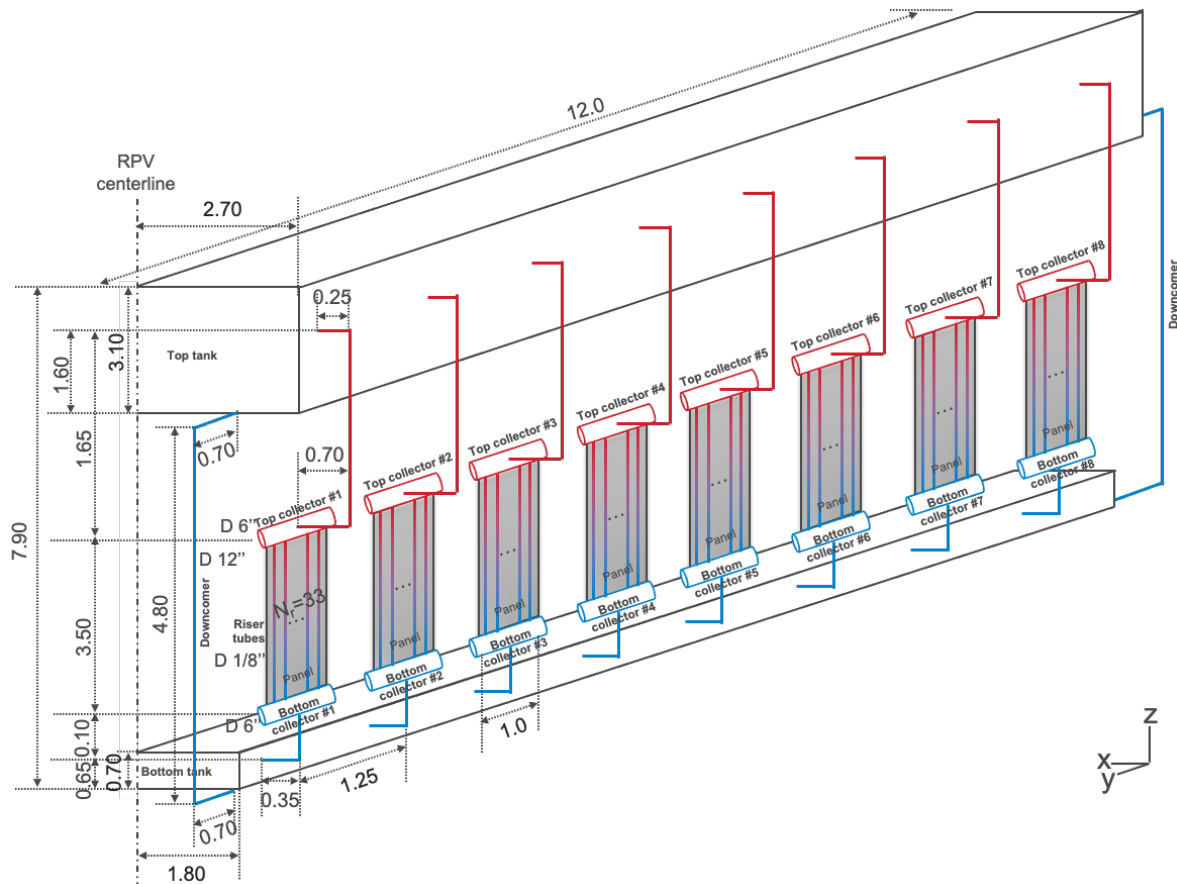


Figure 10 Isometric view of the baseline design of RCCS for HC-HTGR (Not scaled)

3.2.2 Water panel material study

A design perspective on the material selection of the water panel was recommended to be preceded in the initial RCCS design process. Thermal analysis of the water panel was conducted to assess the conduction heat transfer performance by the panel and the riser tube materials using STAR-CCM+ [10]. A test was conducted for a single water panel under the conditions of two constant RPV temperatures, where a calculation domain is shown in Figure 11, and a test matrix is summarized in Table 2. Values of the RPV temperature of 220 °C during the normal operating condition and 472 °C during the limiting design condition were considered to understand the influence on the overall heat transfer path from the RPV to the water panel. It should be noted that those values were approximated to reflect what is expected for a prototypic reactor but not design values exact for the HC-HTGR. The emissivity of the carbon steel was set as 0.8, and emissivity values of 0.3 and 0.1 were used for the stainless steel to investigate the influence of the surface emissivity on thermal performance.

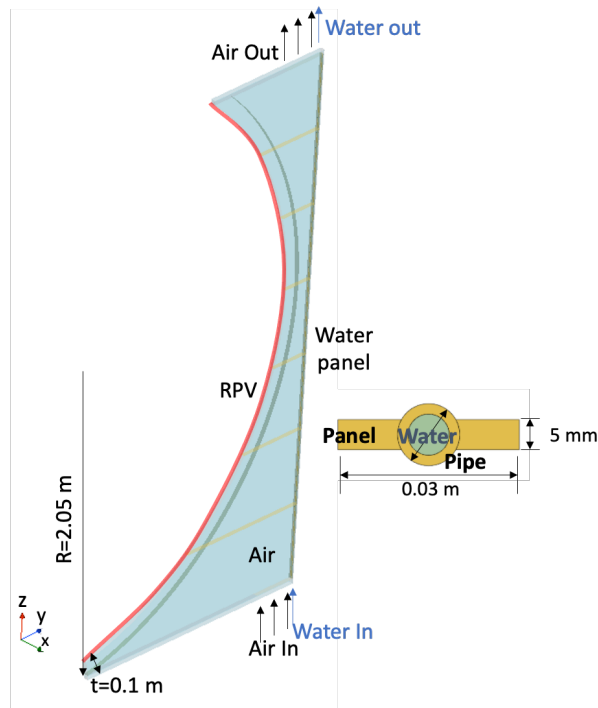


Figure 11 CFD domain of the test case

Table 2 Single water panel conduction performance test matrix

	Boundary conditions	Riser tube material	Emissivity
Case 1-1	Constant $T_{RPV}=220\text{ }^{\circ}\text{C}$	Carbon steel	0.8
Case 1-2		Stainless steel	0.3
Case 1-3			0.1
Case 2-1	Constant $T_{RPV}=472\text{ }^{\circ}\text{C}$	Carbon steel	0.8
Case 2-2		Stainless steel	0.3
Case 2-3			0.1

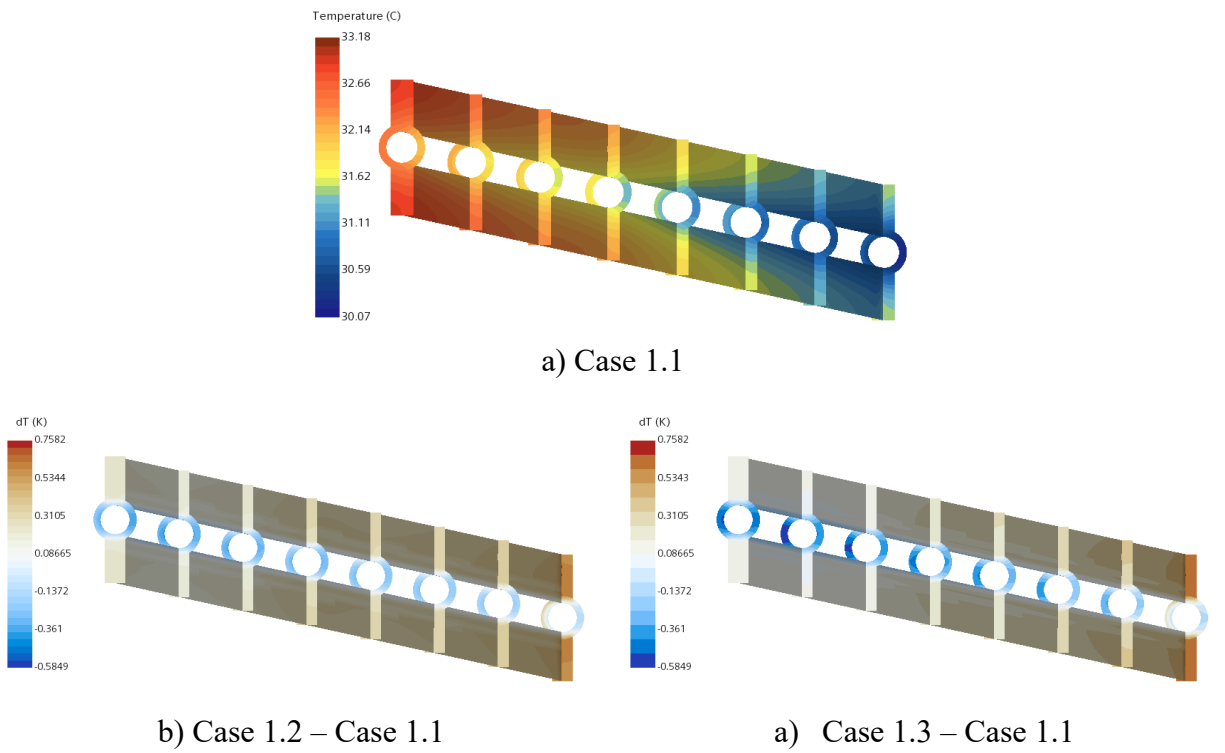


Figure 12 Comparison of the water panel temperature by pipe materials ($T_{RPV}=220\text{ }^{\circ}\text{C}$ condition)

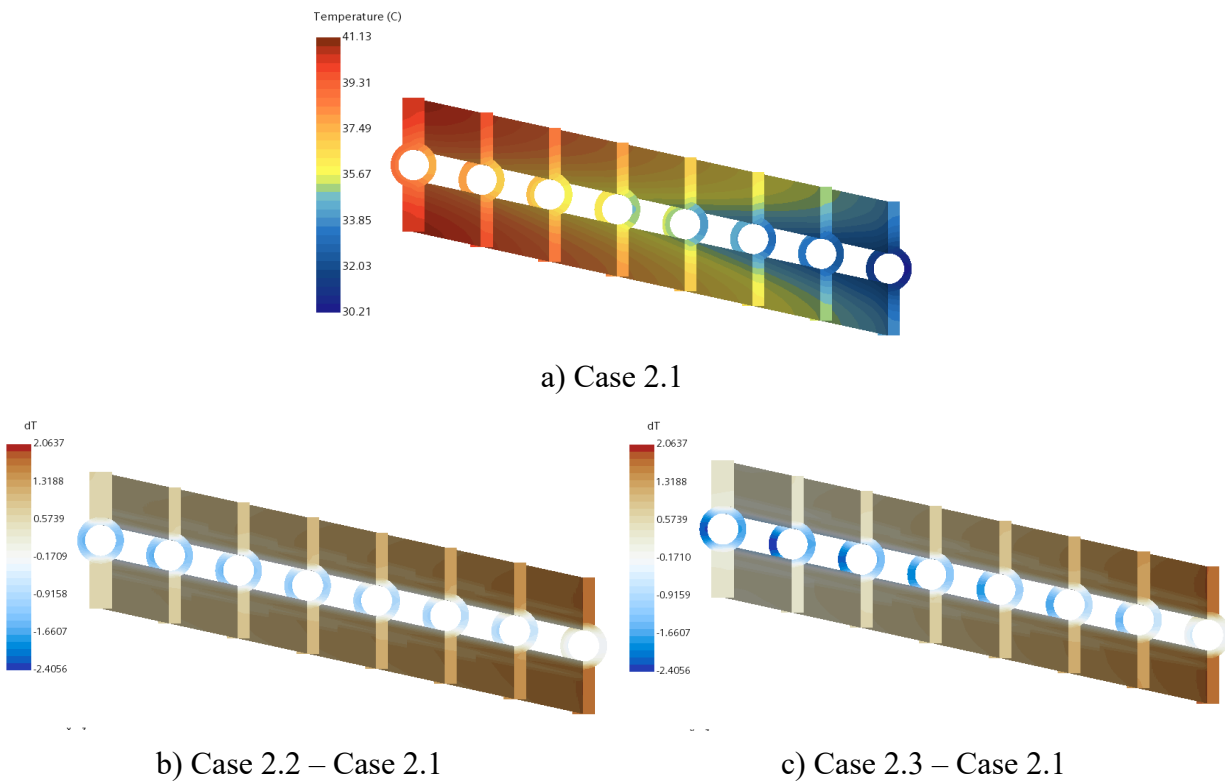


Figure 13 Comparison of the water panel temperature by pipe materials ($T_{RPV}=472\text{ }^{\circ}\text{C}$ condition)

Figure 12 and Figure 13 show CFD-predicted transverse temperature distributions across the water panel by riser tube materials and RPV temperature boundary conditions. The case of stainless steel pipe with the emissivity of 0.3 had the largest temperature gradient on the water panel due to its relatively poor thermal conductivity. The amount of radiation heat transfer from the RPV surface was more shifted to the panel side due to the low emissivity of the stainless steel pipe surface. The panel temperature of the air side of the carbon steel pipe case was slightly larger than those of the stainless steel pipe case. On the other hand, the pipe inner and outer surface temperatures of the stainless steel pipe cases were lower than those of the carbon steel pipe case by on the order of 0.5 - 1.5 °C in the Cases 1.3 and 2.3 respectively. As shown in (b) and (c) of Figure 12 and Figure 13, temperature changes from the carbon steel pipe to the stainless steel pipe with different emissivity values were within a few degrees.

Figure 14 shows a heat flow by the riser tube materials under constant RPV temperature boundary conditions. For the stainless steel pipe case, radiation heat transfer from the RPV surface decreased by up to 22 % in the case of stainless steel pipe with the emissivity of 0.1 compared to the carbon steel case. All cases showed similar level of convection heat transfer of the RPV surface. Heat transfer from the RPV to the water panel was distributed to the panel and the riser tube based on the emissivity. In the carbon steel pipe case, radiation heat transfer from the RPV was shared between the panel and pipe surface area. In contrast, the radiative heat transfer of the stainless steel pipe cases were focused on the panel surface due to its low emissivity. Overall convection heat transfer by water decreased by the reduced amount of radiation heat transfer from the RPV. A slight increment of conduction heat transfer between the panel and the pipe was shown as it had a relatively large temperature gradient between them due to its low thermal conductivity.

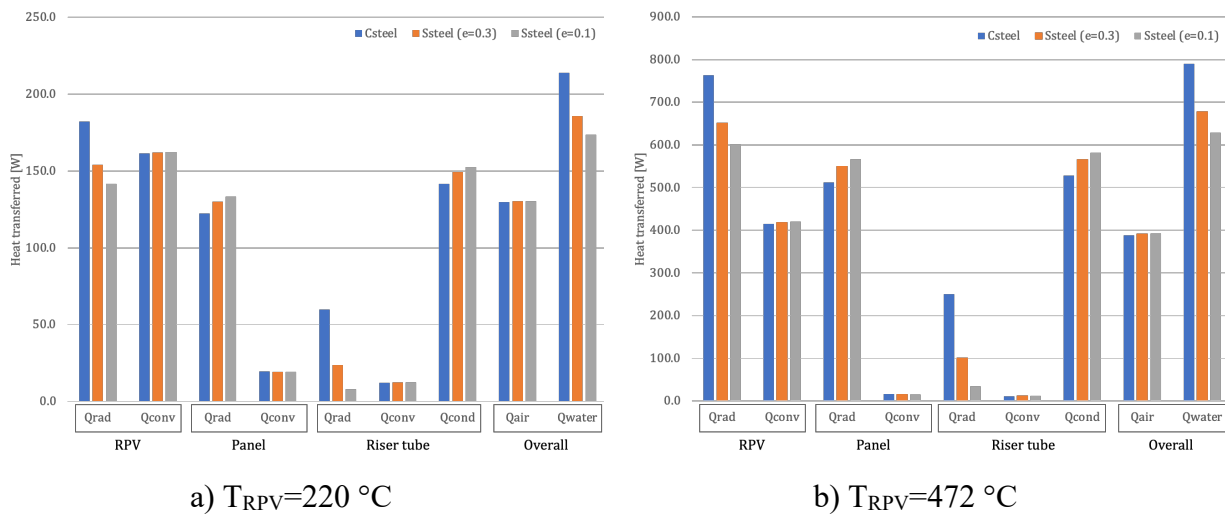


Figure 14 Comparison of heat flow by pipe material in constant temperature boundary conditions

Based on the results, the use of carbon steel for the riser tubes can offer improved heat transfer performance of the water panel when compared against a stainless steel option due higher emissivity and thermal conductivity material properties. Carbon steel is a preferred panel material given its high thermal conductivity and emissivity within the range of 0.7 to 0.9 under most

conditions. For such reasons, carbon steel could be an ideal option for the riser tubes as well as it would simplify fabrication and save construction costs. However, carbon steel has a known corrosion issue and potential long-term structural integrity loss due to the oxidation of chemical reactions with water, as well as degradation of the convective heat transfer and ultimately overall performance of the RCCS. Additionally, the surface will experience loss of material due to this corrosion mechanism and overtime will cause damage due to pitting and erosion [11]. To prevent significant fouling of the fluid and corrosion of the steel piping, it would be necessary to adopt an additional coolant treatment system. In lieu of complex surface treatment and/or stringent chemistry control, stainless steel is commonly chosen instead for piping of the water system. However, the drawback of stainless steel is the relatively poor thermal properties compared to those of carbon steel.

The impact on the overall heat transfer coefficient can be determined based on equation (4), where U_f is the overall heat transfer with fouling, R_f is the fouling factor, and U_c is the heat transfer coefficient of a clean system [12]. One of the primary factors for this high level of fouling is the velocity, which becomes significant at low flow velocities, shown in Figure 15. Furthermore, this rate of heat transfer degradation will continue with to decrease time and is likely to follow either a log or power dependence as shown in Figure 16.

$$U_f = \frac{1}{R_f + \frac{1}{U_c}} \quad (4)$$

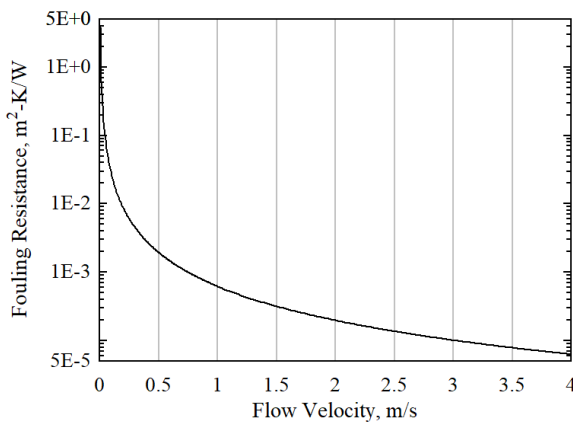


Figure 15 Fouling resistance versus change in flow velocity, based on correlation from [13]

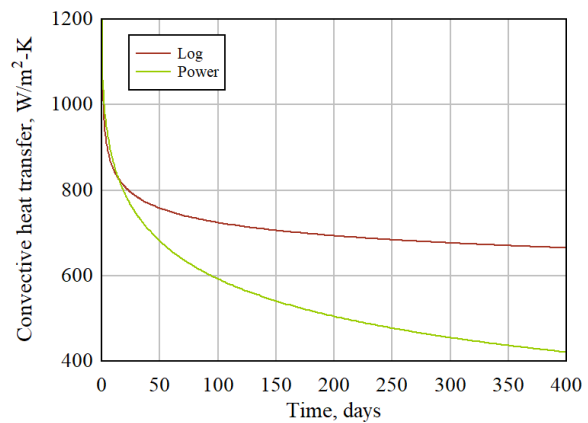


Figure 16 Reduction in heat transfer coefficient assuming log and power trends vs time

Since fouling impacts many applications across various industries, a large amount of work has been completed to identify effective techniques to control against its impact. In cooling water systems, the most common is the addition of chemicals corrosion inhibitors, which form a protective film or barrier on the metal surfaces. This method may impact heat transfer by the fluid

due to film build-up and reduced fluid thermal performance and requires regular monitor to ensure chemical levels are adequate for continued protection. In consideration for possible treatment methods of a water based RCCS, requirements specific to nuclear safety present unique demands and limit the range of viable options. Furthermore, the reliance on natural circulation heat transfer to maintain adequate levels of decay heat removal performance excludes many of the chemical solutions where the build-up of protective film would hinder the convective performance of the cooling panel tubes.

The reduction of dissolved oxygen (DO) is identified as one viable method as it maintains the simplicity in design and operation without chemical or mechanical additives. Removal of DO can be achieved with several techniques, including but not limited to sustained boiling, purging with an inert gas, and sonication. A comparison of these was made by Butlter et al, 1994 [14] and determined that purging with nitrogen gas was the most effective and adequately cost effective for most applications. Though this method would provide acceptable water quality levels initially, ingress of ambient outside air (for example via breather ports for water expansion/contraction in the system) would create a pathway for the reintroduction of oxygen into the system. Thus, additional considerations would need to be made for a continuous and long-term method for maintaining water quality. Possibilities include maintaining a small positive pressure within the gas space above the tank water level, which would create a blanket of cover gas shielding the water surface from the oxygen rich environment. An inert gas such as argon would reduce the amount of gas flow needed to maintain the blanket given the higher density and lower potential for egress by diffusion. Similarly, a slow-flow continuous purge of nitrogen through the piping, etc. gas space may also be able to achieve this goal. Further evaluation of design and operating details would be needed to confirm the effectiveness of such a system, including an assessment of the reliability, long-term operational costs, failure points, and their impacts.

3.2.3 Development of the water panel modeling approach

For the design work for the HC-HTGR RCCS, the RELAP5-3D reactor transient analysis code [15] is being used to investigate the system performance characteristics. Prior to conduct the design calculations, it is important to confirm the system behavior and major heat transfer mechanism of the system can be captured for the design scope. The water panel is a key component of the RCCS to receive the radiation heat from the RPV surface and to remove heat by natural convection of the coolant for the RCCS, therefore, a conventional modeling approach using RELAP5-3D have been revisited. To properly organize the heat structures of a pipe with a fin (known as a panel) in the reactor cavity in RELAP5-3D, modeling assumptions are necessary due to the complex geometry and constraints of the code when considering combined heat transfer mechanisms involving radiation and conduction within the same structures. One surface of a heat structure in RELAP5-3D cannot be specified in more than one enclosure set. It indicates modeling heat transfer surfaces of the pipes with fins including both radiation and conduction heat transfer are not available, therefore, it requires proper assumptions in heat structures and their heat transfer modeling to reflect major thermal responses expected in RCCS operation.

Figure 17 shows a comparison of the water panel modeling approach in RELAP5-3D by modeling assumptions made in the heat structures of the panel and the pipe. As the radiation heat transfer is known to be the dominant heat transfer mechanism of typical situations of HTGR, the radiation enclosure has been preferred and defined in the input by combining pipes and fins into a

single heat structure in previous studies [9,16] as shown in Figure 17 (a). Although thermal conduction heat transfer between pipes and fins is not included with that, the total energy balance within each structure would be conserved with proper corrections such as adopting a fouling factor for a heat transfer coefficient. However, this approach might require lots of assumptions made in the water panel modeling in defining representative material properties if the panel and the pipe materials are different, or complex geometries of the panel and/or the riser tubes.

Therefore, it leads to complementing the traditional modeling approach for the water panel to incorporate all important heat transfer mechanisms while conserving important physical parameters such as geometries and dimensions. An extended modeling approach is developed by modeling the panel and the riser tube exclusively and setting each surface of heat structures within a radiation enclosure, while the other side of heat structures are jointed within a conduction enclosure simultaneously as shown in Figure 17 (b). It enables to thermally connect the panel and the riser tube through conduction and radiation enclosures simultaneously. In other words, the side facing the gap of heat structure surface is set in radiation enclosure. Then the opposite side of heat structure surface is included in the conduction enclosure at the same time, while the actual thermal conduction between the panel and the riser tube occurs at the side. This approach might bring modeling complexities in defining heat structures and thermal conductions, but it is expected to reflect the actual heat transfer mechanisms expected in RCCS operation condition to the best extent.



Figure 17 Schematics of RELAP5-3D modeling approaches of the water panel

A test case was prepared to assess modeling approaches for the water panel using RELAP5-3D, and the results of each approach were compared with CFD simulations. The geometry of the test case represents the unit geometry of the HC-HTGR RCCS design. The test case includes a part of a horizontal RPV surface, a straight vertical panel and pipe assembly, the air between the RPV and the panel/pipe assembly, and water flowing in the pipe. To limit the calculation domain, the air and the water flows were modeled as once-through with fixed inlet temperature and flow rate, while water flow is in a closed loop driven by natural circulation in the actual operation. Specifications of the RELAP5 test case are listed in Table 3. Note that values of the mass flow rate of the air and the water are not representing specific design values but are set with approximated values for the test purpose.

Table 3 Dimensions of the RELAP5 test case

Parameters	Values
RPV outer diameter	4.1 m
RPV/panel/riser tube height	3.5 m
RPV/panel width	0.03 m
RPV thickness	0.1 m
Pipe inner/outer diameters	0.269 inch / 0.405 inch (1/8 inch standard Sch. 40 pipe)
Water inlet temperature / mass flow rate	30 °C / 0.03 kg/s
Gap air inlet temperature / mass flow rate	65 °C / 0.05 kg/s

A simplified nodalization diagram of each modeling approach is presented in Figure 18. It consists of two hydrodynamic volumes for the coolant (water) and the gap (air), and heat structures for the RPV surface, the panel and/or the riser tube, top/bottom structures to close the volume (not shown in Figure 18), and time dependent volumes and junctions to define boundary conditions of the fluid domain. Hydrodynamic components and heat structures such as RPV surface, top and bottom structures were shared for the inputs of both approaches. The water coolant was modeled with a vertical pipe component (101) with 7 axial nodes. The cavity, the space between the RPV and the panel, was modeled with a vertical pipe component (220) with 7 axial nodes and with another hydrodynamic system considering non-condensable gas present environment such as air. As flow area of the cavity varies by its elevation, flow area, length, and hydraulic diameter (D_h) set in the input were processed from the volume of actual geometry for each axial node with consideration of their azimuthal angle to reflect actual geometry of the air domain to the best extent. The RPV surface was represented with a rectangular geometry heat structure (HS 2201). Thickness of the RPV heat structure was set as 0.1 m for all axial nodes, varying surface area of each axial node with elevation to model curvatures of them. Top and bottom structures were modeled as rectangular heat structures with single axial node as they are required to complete enclosure of the calculation domain for calculating radiation heat transfer. They do not affect the temperature distributions of any heat structures as no thermal connections were set with other heat structures, nor thermal radiational heat taken by setting emissivity values for the top and the bottom heat structure surfaces as zero.

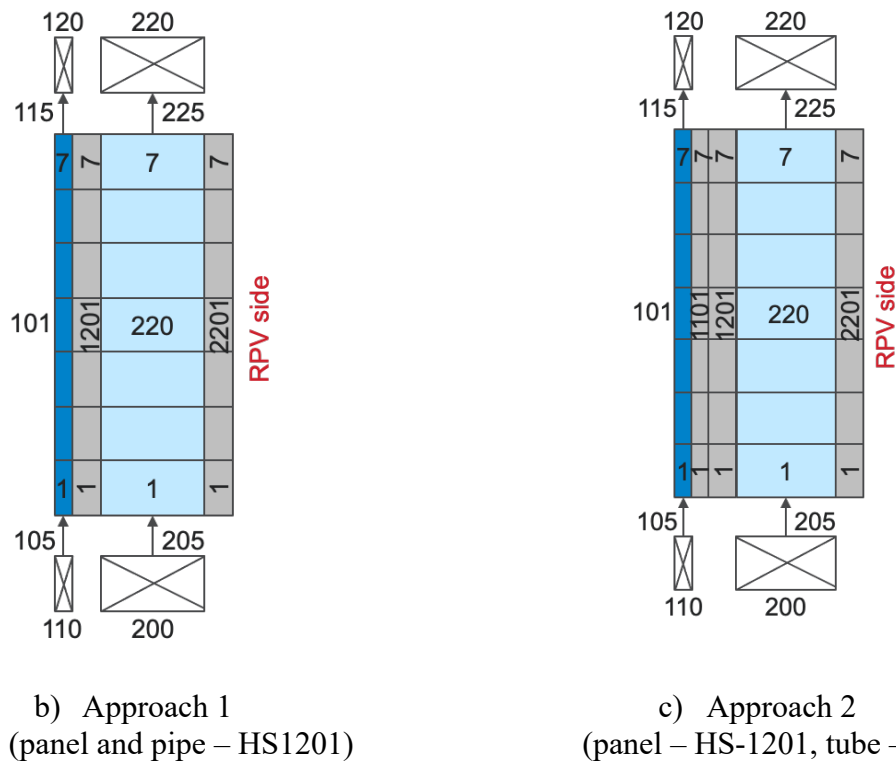


Figure 18 RELAP5-3D nodalization diagram of the test case by the modeling approach

Heat structures for the panel and the tube were varied according to assumptions made in the modeling of the water panel. For Approach 1, the panel and the pipe were modeled as a single rectangular heat structure (HS 1201) having 7 axial nodes, where the panel and the pipe surface area on the cavity side was conserved but its curvature was ignored. As rectangular heat structure in RELAP5-3D has same surface area for the left and right sides, the left side area connected to the water were overestimated. To account for the difference between the defined surface area (A_{relap}) and the actual pipe inner surface area ($A_{pipe,in}$) contact with the water, a correction was made by using a user-defined convective heat transfer coefficient multiplier, Fouling factor (F), to adjust the total left side heat transfer as equation (6), where $F=0.60$ was set in the test case.

For Approach 2, the panel and the pipe were modeled as rectangular heat structures (HS-1201 and HS-1101) with both having 7 axial nodes. Note that the thickness of the panel and the pipe and the surface area of the panel were exact values of actual geometry but not for surface area of the pipe, as the pipe was modeled as flat plate which has same surface areas for left and right boundaries and surface area value was picked for the air side surface area. This discrepancy of surface area, especially for the water side, will require a proper correction of heat transfer. As done in the Approach 1, it was achieved by using a Fouling factor (F) to adjust the total left side heat transfer as equation (6), now $F=1.33$. To take into account of conduction heat transfer between the panel and the pipe, a gap conductance (K) was corrected for a set of conduction enclosure. A correction was made to account for the actual contact area between the panel and the tube ($A_{contact}$) in a gap conductance (K) for a set of the conduction enclosure as equation (7), where k is the thermal conductivity of the heat structure material assuming a constant value (47.7 W/m K for

carbon steel), and L_{cond} is the conduction length, respectively. For the test case, $K=988.6 \text{ W/m}^2\text{K}$. Detailed comparison of heat structure inputs for the panel and the pipe by RELAP5-3D modeling approach are summarized in Table 4.

$$F = A_{pipe,in}/A_{RELAP} \quad (6)$$

$$K = \frac{A_{contact}}{A_{RELAP}} * \left(\frac{k}{L_{cond}} \right) \quad (7)$$

Table 4 Specifications of the panel and the pipe heat structure inputs by the modeling approach

	Approach 1	Approach 2	
Heat structures	Panel & pipe (HS-1201)	Panel (HS-1201)	Pipe (HS-1101)
Shape	Flat plate	Flat plate	Flat plate
Thickness	5 mm	5 mm	1.727 mm
Left boundary condition	Convective (water)	Symmetry & Set in conduction enclosure	Convective (water)
Right boundary condition	Convective (cavity)	Convective (cavity) & Set in radiation closure	Symmetry & Set in conduction enclosure

RELAP5-3D simulation results of all approaches were compared with CFD simulation results under the same boundary conditions. CFD results were post-processed by using reports taking surface/volume average or integral to directly compare with physical quantities of RELAP5-3D results such as node temperature, heat structure surface temperature, heat transfer amount, etc. A constant RPV inner temperature of 220 °C was used for the boundary conditions, intended to be a reference in estimating a parasitic heat loss by RCCS during normal operational conditions in system scale analysis.

Table 5 and Table 6 summarize comparisons of heat flow by RELAP5-3D modeling approach with CFD results in constant RPV temperature of 220 °C and 472 °C conditions, respectively. Both approaches predicted radiation heat transfer and convection heat transfer from the RPV at a similar level to CFD results in two RPV temperature cases. It was noticeable that with proper corrections made from the modeling assumptions for the major components, all approach reasonably agrees well with CFD results. As some axial nodes of the RPV used their heat transfer correlations for a flat plate to reflect their curved geometries, minor discrepancies in heat transferred by the air flow could be reduced by updating proper heat transfer coefficient correlations for them once system configurations and dimensions are finalized.

Table 5 Comparison of the test case results of RELAP5-3D and CFD - $T_{RPV}=220\text{ }^{\circ}\text{C}$

	RELAP5-3D		CFD
	Approach 1	Approach 2	
Total heat transfer [W]	348.38	348.09	343.54
Radiation heat transfer [W]	188.35 (54.1 %)	188.07 (54.0 %)	182.16 (53.0 %)
Convection heat transfer [W]	160.03 (45.9 %)	160.03 (46.0 %)	161.38 (47.0 %)
Heat transferred by air [W]	112.82 (32.4 %)	113.08 (32.5 %)	129.70 (37.8 %)
Heat transferred by water [W]	235.55 (67.6 %)	235.02 (67.5 %)	213.85 (62.2 %)

Table 6 Comparison of the test case results of RELAP5-3D and CFD - $T_{RPV}=472\text{ }^{\circ}\text{C}$

	RELAP5-3D		CFD
	Approach 1	Approach 2	
Total heat transfer [W]	1183.14	1188.40	1178.82
Radiation heat transfer [W]	794.50 (67.2 %)	792.70 (66.7 %)	763.61 (64.8 %)
Convection heat transfer [W]	388.64 (32.8 %)	395.70 (33.3 %)	415.21 (35.2 %)
Heat transferred by air [W]	338.85 (28.6 %)	355.03 (29.9 %)	388.56 (33.0 %)
Heat transferred by water [W]	844.29 (71.4 %)	833.37 (70.1 %)	790.26 (67.0 %)

From the comparison of test case results, all modeling approaches predictions agreed reasonably well agreed with CFD results with proper corrections on heat transfer area for thermal radiation or conduction. They were made from different levels of assumptions in the inclusion of heat transfer mechanism and physical parameters. Previous studies and extensive experiences have been done with Approach 1 with its straightforward concept and simplicity of modeling. They showed it would be suitable for analyzing the panel and the pipe in the same material. Approach 2 is the extended version of Approach 1 but explicitly modeling the panel and the pipe. It is recommended for analyzing a case of dual materials of the panel and the pipe or transient analysis such as drastic changes in heat source or flow rate of the water and/or cavity, etc. It has a potential to reflect thermal responses of each component in different material in transient condition. Therefore, Approach 2 was used to first develop the RELAP5-3D reference model for the HC-HTGR RCCS design study, but Approach 1 could be coming along with Approach 2 if necessary.

3.2.4 Preliminary performance analysis of the HC-HTGR RCCS

The pre-conceptual design of the HC-HTGR RCCS consists of 8 riser tube assemblies, where each has 33 riser tubes connected with the panel and connecting to top and bottom collectors on each side of the RPV. For system redundancy, top and/or bottom tanks could have multiple compartments to make an independent train for system operation. In the preliminary analysis model, 1/8th volume of total top and bottom tanks with a single rise tube assembly was firstly considered to estimate system performance. Figure 19 shows the RELAP5-3D model for the 1/8th compartment of the pre-conceptual design of the HC-HTGR RCCS natural circulation loop. Along with the natural circulation loop, air flow between RPV and the water panel was modeled. Since the reactor building's internal configurations was not yet finalized, the air flow was modeled with a fixed flow rate and inlet temperature through the gap with approximated values in the present model, which are 30 °C and 0.48 kg/s respectively. The detailed descriptions of the RELAP5 model are available in [17].

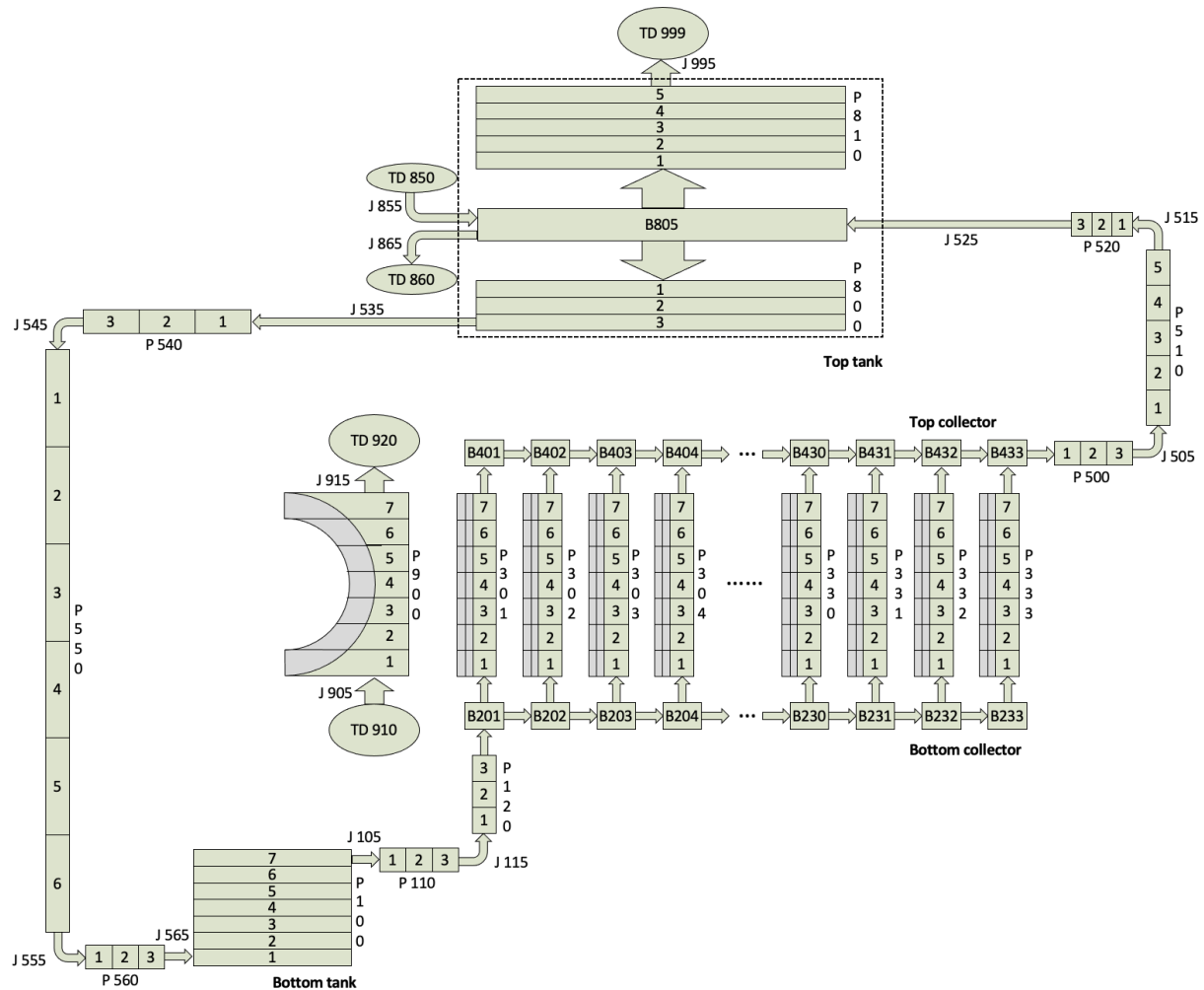


Figure 19 Nodalization diagram of the RELAP5-3D model for the pre-conceptual RCCS design [17]

Table 7 shows the preliminary results on the performance of the pre-conceptual design of the HC-HTGR RCCS under conditions of the top tank exit temperatures of 30 °C and 80 °C in normal operating and limiting design conditions. In the normal operating condition, a temperature rise from cold leg entrance to hot leg return was from 6 to 15 °C, which indicated the system operation range were in a subcooled state with a proper top tank cooling. The 80°C top tank case in the limiting design condition showed a coolant temperature rise by 20.7 °C. The coolant exit temperature of the riser tube was a few degrees below saturation temperature. A larger heat load of the RCCS water panel was predicted in the 30°C top tank case than that of the 80 °C top tank case in both conditions. In the limiting design condition, the RCCS water panel load increased up to 72.1 % in the 30°C top tank case. It confirmed the major heat transfer path from the RPV to the water panel was radiation. Parasitic heat loss from the RPV in the normal operating condition could be estimated by converting 1/8th of compartment results into a full system heat load. Multiplying 16 to the heat removal from RPV per single riser tube assembly, 0.17 MW_t and 0.13 MW_t for the 30°C and 80°C top tank temperature cases were predicted in normal operation conditions. This satisfied maintaining below target maximum heat loss during normal operation by the HC-HTGR RCCS operation. However, the heat removal rate under the limiting design condition was estimated to 0.56 MW_t for the 30 °C top tank condition, which is below the design target of 1 MW_t for the HC-HTGR RCCS.

Table 7 Performance of 1/8th compartment of the pre-conceptual RCCS design

	30 °C top tank	80 °C top tank
Normal operation condition (T_{RPV}=220 °C)		
Coolant temperature rise [°C]	14.28	6.03
Total mass flow rate [kg/s]	0.09831	0.1341
Heat removal from RPV [kW]	10.65	8.189
RCCS water panel heat load [kW]	5.87 (55.1 %)	3.40 (41.5 %)
Limiting design condition (T_{RPV}=472 °C)		
Coolant temperature rise [°C]	27.70	20.67 (T _{sat} =108.4 – 114.1 °C)
Total mass flow rate [kg/s]	0.2181	0.2253
Heat removal from RPV [kW]	35.03	28.93
RCCS water panel heat load [kW]	25.24 (72.1 %)	19.58 (67.7 %)

3.2.5 Design parametric study of the HC-HTGR RCCS

Followed by the preliminary analysis, the approximated thermal performance of the pre-conceptual RCCS design in the limiting design condition was insufficient. It led the major design update for the pre-conceptual design of the HC-HTGR RCCS to achieve the system target performance of 1 MW_t. In addition, the heat loss by the gap air flow was excluded to be conservative in the RCCS design process, which assisted ~28 % of total heat removal from the RPV. Therefore, the reference design conditions for the HC-HTGR RCCS considered in the design parametric analysis were revised per request as below:

- Average RPV surface temperature of constant 420 °C
- The emissivity of 0.8 for all surfaces participating in radiation heat transfer
- Single-phase operation with higher water temperature throughout the loop
- Air convection at both RPV outer surface and water panel surface is ignored.
- Thermal radiation heat transfer from the water panel to the cavity concrete wall is ignored.
- Radiative heat transfer between the RPV and top and bottom tanks is ignored.

Under such design constraints and reference design conditions for the RCCS of HC-HTGR, prioritized strategies to improve the thermal performance of the water panel were addressed with the aim of maximizing the water panel surface area and minimizing loss of radiation from the RPV to environment/structures other than the water panel. An attempt (Attempt 1) was made to find the design of the water panel to achieve the target heat removal rate within a limited vertical elevation change allowed to the water panel. Figure 20 and Table 8 show the variations of the water panel design of HC-HTGR RCCS considered. Under the pre-conceptual RCCS system configuration, it was inevitable to increase the width of the water panel to maximize its surface area. By increasing the number of the riser tube per water panel and extending water panel to cover the RPV at the best extent, another design (Attempt 2) had 1.1 MW of the heat removal performance in the design condition. However, it was obviously violating design requirements as interfering with the vertical supports and not allowable as it was limited it to 1.0 m to leave the design space for the vertical supports.

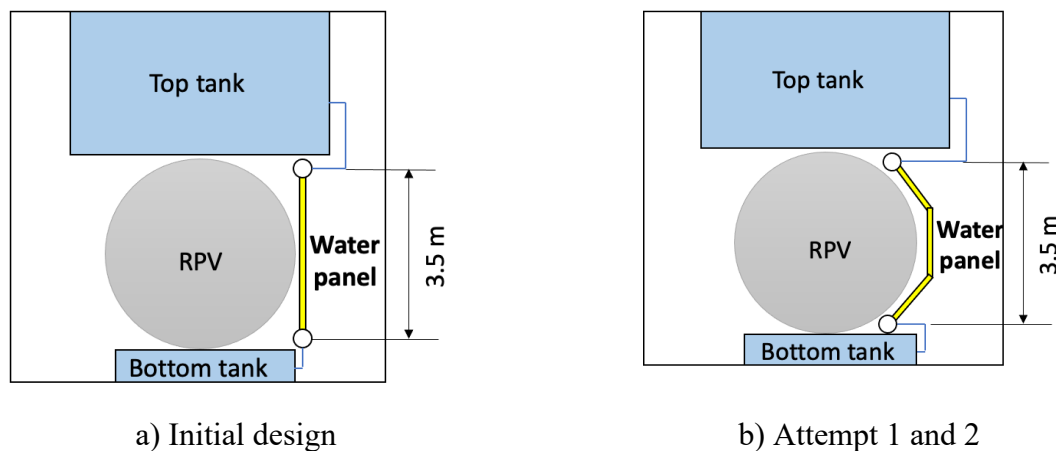


Figure 20 Major design changes of the water panel of HC-HTGR RCCS (Not scaled)

Table 8 Comparison of the water panel design performance

	Baseline	Attempt 1	Attempt 2
Riser tube diameter	1/8 inch (Sch. 40)	1/8 inch (Sch. 40)	1/8 inch (Sch. 40)
Number of water panel	8 on each RPV		
The number of riser tubes per water panel	33	66	66
Width of a water panel	1.0 m	1.0 m	1.5 m
Riser tube P/D	2.92	2.19	2.19
Shape	Vertical, straight	Partially inclined	Partially inclined
Vertical elevation	3.5 m	3.5 m	3.5 m
Total heat removal rate in the design condition*	0.56 MW	0.85 MW	1.10 MW

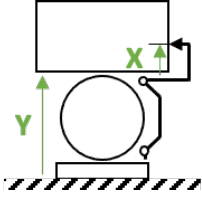
* Evaluated with the single riser tube and scaled to the full system

A design parametric study was continued to find the design of the water panel and the loop configuration satisfying the design goal of the RCCS under the design condition. For the modified water panel design (Attempt 1), top tank injection elevation (X) and the top tank elevation (Y) were investigated with a unit water panel having a single riser tube model using RELAP5-3D. Table 9 shows the summary of the RCCS performance by natural circulation loop configurations. 1.0 m is the maximum allowable margin for both the top tank elevation to be located inside the reactor building and for the top tank injection elevation to have at least 30 % of the level of the top tank water inventory as the depletion state from the given top tank size. As expected, the two parameters brought a favorable impact on promoting natural circulation flow rate, but they had insignificant enhancement of overall thermal performance. This indicated that the system performance evaluated in the design condition was primarily limited by the thermal radiation from the RPV.

For a cylindrical shell shaped water panel with a smooth surface covering the entire RPV area, radiation heat transfer from the RPV can be calculated by equation (8) **Error! Reference source not found.**, where ϵ is the emissivity, σ is the Stephan-Boltzman coefficient ($5.67 \times 10^{-8} \text{ W/m}^2\text{K}^4$), A is the surface area, and D is the diameter [8]. It was estimated that 0.95 MW_t could be achieved in the design condition with a panel temperature of $65 \text{ }^\circ\text{C}$ and an emissivity of 0.8, which is close to the target thermal performance of the HC-HTGR RCCS design.

$$Q_{RPV} = \frac{\epsilon_{RPV} \sigma A_{RPV} (T_{RPV}^4 - T_{panel}^4)}{\left[\frac{1}{\epsilon_{RPV}} + \frac{1 - \epsilon_{panel}}{\epsilon_{panel}} \left(\frac{D_{RPV}}{D_{panel}} \right) \right]} \quad (8)$$

Table 9 Thermal performance by top tank injection elevation (X) and top tank elevation (Y) in the design condition

		Ref.	Top tank injection elevation (X)			Top tank elevation (Y)		
			+0.2 m	+0.6 m	+1.0 m	+0.2 m	+0.6 m	+1.0 m
Radiation [W]	From RPV	1066.1	1066.4	1067.0	1067.5	1066.4	1067.0	1067.5
	To structures	432.6	432.6	432.5	432.4	432.6	432.5	432.4
	To riser tube outer surface	305.8	305.9	306.2	306.4	305.9	306.2	306.4
	To panel	404.9	405.1	405.5	405.8	405.1	405.5	405.8
Mass flow rate [kg/s]		6.0e-3	6.2e-3	6.4e-3	6.7e-3	6.2e-3	6.4e-3	6.7e-3

It was confirmed the main design parameter of the RCCS is the water panel surface area. Since the RPV side surface covered by the water panel was partially blocked by the top and bottom tanks for the pre-conceptual design, it limited the heat transfer from the RPV to the water panel. By locating the top tank to the position other than above the RPV, it was expected to improve the thermal performance of the RCCS. It was expected to utilize additional RPV area participating in radiation heat transfer to the water panel and minimize heat loss to the structures simultaneously. It also allowed extending a height of the water panel to promote the natural circulation flow.

To support the changes in top tank configuration, transient simulations were conducted using RELAP5-3D. The results of two cases were compared – one is the top tank is isolated and not receiving any radiation heat transfer from the RPV (Case 1), and the other is the top tank surface adjacent to the RPV receives the radiation heat transfer from the RPV directly (Case 2). The transient scenario considered for the analyses is the hypothetical Depressurized Conduction Cooldown (DCC) event, which adopted the RCCS heat load evolution by time from a reference HTGR design [18]. The power profile was normalized to have a designed power level of HC-HTGR and set as a heat flux boundary condition at the RPV inner surfaces. Started with the steady state natural circulation operation condition starting from 0 sec, heat sink for the top tank temperature was assumed unavailable. The simulation was conducted for the initial 300 hours to investigate the impact of the heat loss to the structures such as the top tank to the system behavior.

Figure 21 shows the comparison of the RPV temperature and natural circulation flow rate of evolutions during DCC for the Cases 1 and 2. Both cases showed the peak RPV temperature after ~120 hours, and its differences between two cases was insignificant. However, the case 1 had the maximum RPV temperature at the center as the top tank is isolated with the RPV, while case 2 did at the top of the RPV. With continuous heating of the top tank by thermal connection with the RPV, Case 2 had a lower natural circulation flow rate and faster system heating up with earlier

boiling incipient than that of Case 1. The results supported the top tank layout change to avoid the potential heat transfer to the top tank or any structures near the RPV which suppress the heat transfer and accelerate the inventory of the system inventory boiled-off.

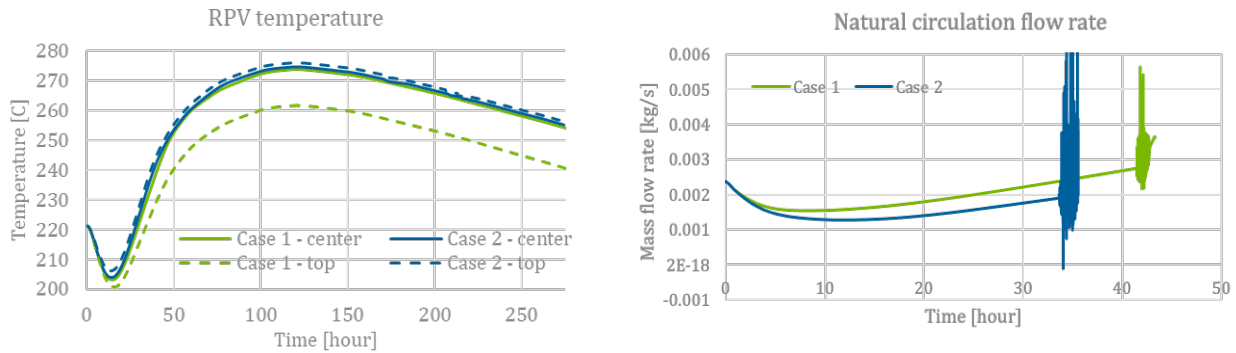


Figure 21 The RPV temperature and natural circulation flow rate during DCC (natural circulation flow rate after boiling mass flow rate was omitted.)

Afterwards, an updated design of the vertical supports for the RPV was potentially considered by the project team after design iterations. By reducing the number of vertical supports to two on each RPV side and locating them at both ends of the RPV in the axial direction as shown in Figure 22, any restriction of heat transfer area of the RPV to the RCCS water panel from the vertical supports would be minimized. This change allowed considering the reference elevation of the top tanks above the RPV, so the top tanks are still located in the reactor building in the current reactor design stage [19] with maintaining compact layout of the RCCS components in the reactor building.

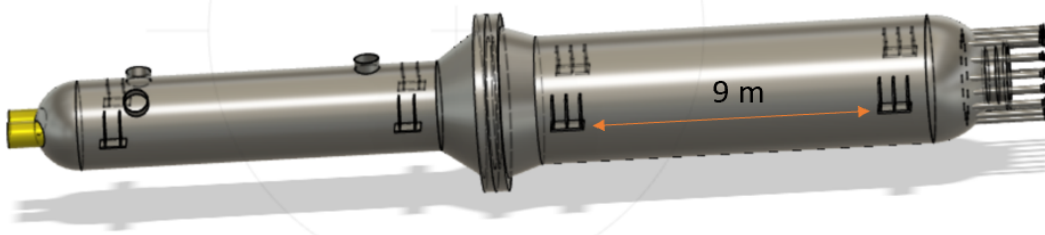


Figure 22 Potential design updates of the vertical supports for the HC-HTGR (as of Dec. 2022, provided by Boston Atomics.)

With the changes in design requirements from the vertical supports design updates regarding mechanical interfaces with the system, the major design parameters on the natural circulation loop have been revisited by standalone RCCS analysis described in the section 3.2.1. In addition, it was noted by the project team that the initial baseline design of small diameter riser tubes and thin panel might have unfavorable features in fabrication and structural rigidity and the riser tube

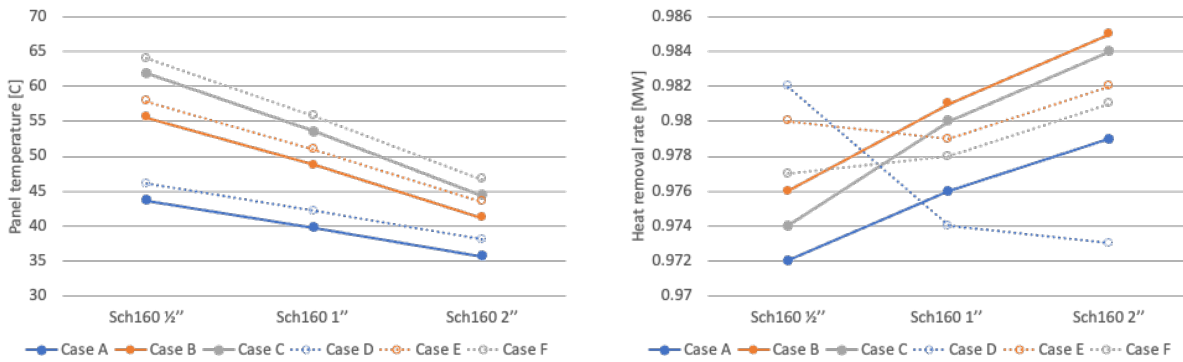
channel might be easily blocked during system operation. A design parametric analysis was conducted under the design condition by varying P/D from 2.2 to 5.0, riser tube diameter with higher grade (from Sch. 40 to Sch. 160) from 1/2 inch to 2 inch, and panel thickness from 5 mm to 20 mm by the standalone RCCS analysis, where the test matrix is summarized in Table 10.

Table 10 Updated design parametric test matrix for the water panel

		Riser tube specifications	t_{panel} [mm]	P/D	# of riser tubes (per single panel)
Initial baseline		Sch 40 1/8 inch	5	2.2	397
A	1	Sch 160 1/2 inch	5	2.2	191
	2	Sch 160 1 inch			153
	3	Sch 160 2 inch			122
B	1	Sch 160 1/2 inch		4.0	105
	2	Sch 160 1 inch			84
	3	Sch 160 2 inch			66
C	1	Sch 160 1/2 inch		5.0	84
	2	Sch 160 1 inch			67
	3	Sch 160 2 inch			53
D	1	Sch 160 1/2 inch	20	2.2	191
	2	Sch 160 1 inch			153
	3	Sch 160 2 inch			122
E	1	Sch 160 1/2 inch		4.0	105
	2	Sch 160 1 inch			84
	3	Sch 160 2 inch			66
F	1	Sch 160 1/2 inch		5.0	84
	2	Sch 160 1 inch			67
	3	Sch 160 2 inch			53

Figure 23 shows the panel temperature and the heat removal rate by the riser tube diameter for various panel thickness and P/D. For all cases (Case A to F), the larger diameter riser tube case showed lower panel temperature as having higher natural circulation flow rate with less frictional loss. For the same riser tube diameter, it had higher panel temperature as P/D and the panel thickness increased. It had a clear trend of the panel temperature by the riser tube diameter, P/D, and the panel thickness. The overall heat transfer performance was determined by a balance

between the natural circulation flow and the water panel surface area. The heat transfer rate was dependent on the surface area of the water panel with larger riser tube diameter in all thin panel cases (Case A to C). On the other hand, a low P/D case of the thick panel case (Case D) had lower thermal performance with larger riser tube diameter, while a high P/D case of the thick panel case (Case F) showed the opposite. It should be noted that the overall heat removal rate was in a similar level for all cases under consideration. It supports to update the water panel design having favorable features in engineering aspects by increasing the riser tube diameter with a higher grade and thick panel.



a) Panel temperature

b) Heat removal rate

Figure 23 Updated design parametric study results

Based on the results and the engineering judgement by the project team, the updated RCCS with the new water panel design has been derived as shown in Figure 24. Satisfying all updated design requirements, it has the same top tank vertical elevation located in the reactor building and same elevation from the bottom of the top tank to the injection. A distance between the RPV and the water panel was also maintained to 0.1 m. The bottom tank was replaced to the header to have the same function, and the top tank above the RPV was divided into two tanks and relocated to the top corner of the reactor building. With the changes made for the top and bottom tanks, the water panel had 165 % of area increase to cover more RPV area including top and bottom regions where those were previously blocked by the tanks. In spite of the changes, it composes a compact system configuration but has better heat transfer performance. In the design condition, 0.99 MW_t of thermal performance is expected with the enhanced natural circulation flow rate, where the performance is summarized in Table 11.

4 A Conceptual Design of the HC-HTGR RCCS

Based on the design process of the HC-HTGR RCCS described in Section 3, the conceptual design of the HC-HTGR RCCS has been developed focusing on the natural circulation loop portion and system components of the system. This section will describe the conceptual design of the HC-HTGR RCCS including the system configuration, key system components, and system operating mode considered in the current design stage.

4.1 Design descriptions

The HC-HTGR RCCS is a water-based natural convection operated system. It comprises of two independently operating loops. Each has a single water panel located at each side of the RPV, a top tank, and connection piping to close the loop and has a symmetric configuration with the RPV at the center. A series of riser tubes is arranged in a single water panel. Water coolant in each loop is heated by direct radiation heat transfer from the RPV to the water panel, which drives circulation from the water panel to the tank through upper collectors and hot legs. During normal operation, water in the tank is cooled by other means, such as an immersed air or water-cooled heat exchanger, which type would be determined in future. Then, the water returns to the water panel through downcomer and cold leg. The current conceptual RCCS design has been characterized to have 11 segments of upper and lower collectors. Each segment holds six riser tubes per segment. Two downcomers are connected per tank, where piping details and the number of the downcomer might be further updated by the number of top tank segments and reactor internal structures design by the project team. Figure 25 and Figure 26 show schematics of the loop configuration and dimensions of the conceptual design of the HC-HTGR RCCS.

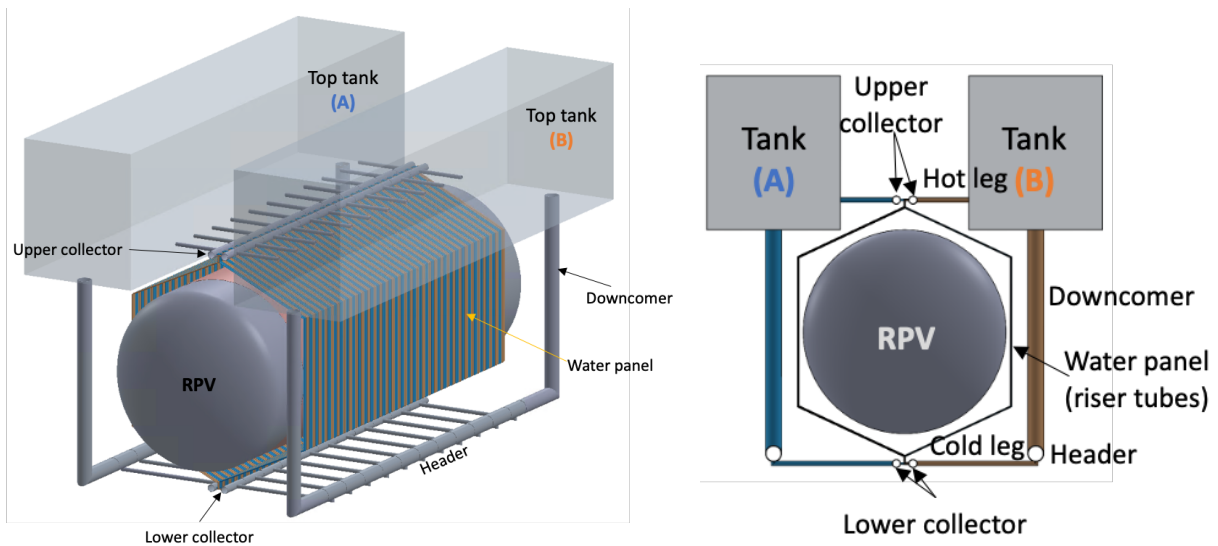


Figure 25 A system configuration of the conceptual design of the HC-HTGR RCCS

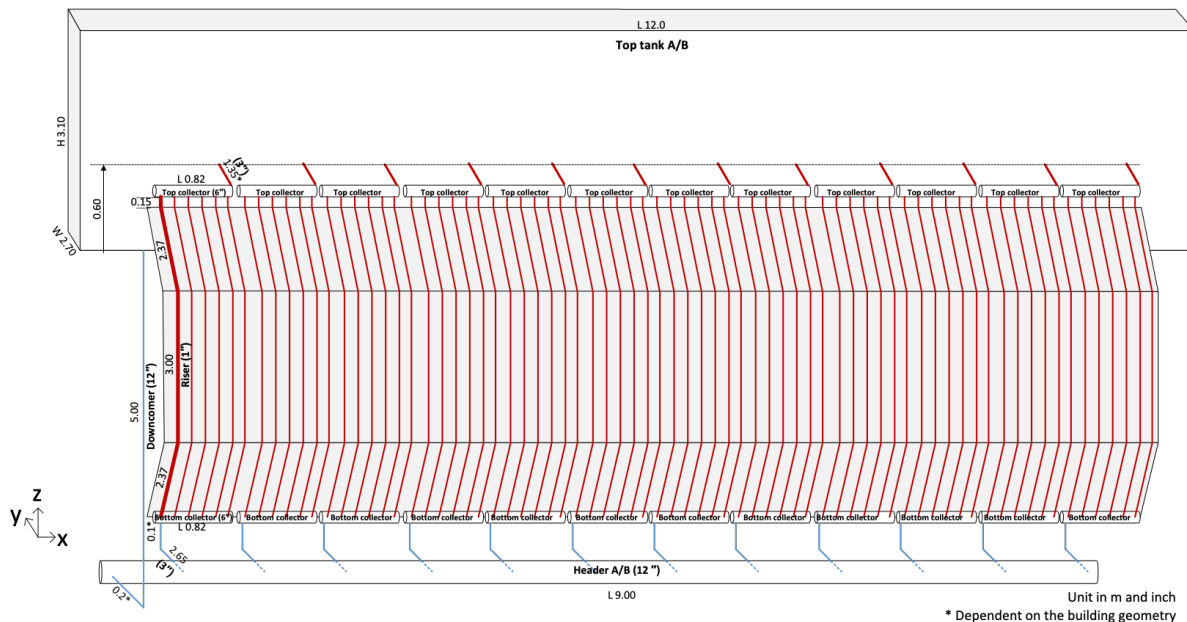


Figure 26 Dimensions of the conceptual design of the HC-HTGR RCCS (not scaled, single loop)

4.2 Key system components

The water panels of the RCCS for the HC-HTGR consist of a series of parallel tubes called riser tubes connected to each other by carbon steel plate called panel. The water panel surface is located 0.1 m apart from the surface of the RPV at the center elevation of the RPV. The water panel has 115-degree angled surfaces at the top and bottom, and the middle part is vertical with a height of 3 m with total vertical height of the water panel is 5.0 m. Total of 66 of Sch. 160 1-inch carbon steel riser tubes are arranged with a pitch-to-diameter (P/D) ratio of 4.0 connected with the 10-mm thick carbon steel panel. The reference emissivity for the water panel is 0.8 which can be achieved through surface treatment of the base material. Key dimensions of the water panel of the HC-HTGR RCCS are summarized in Table 12.

Table 12 Specifications of the water panel of the conceptual HC-HTGR RCCS design

Parameters	Values
Number of water panels	1 at each RPV side (total 2)
Width of single water panel	9.0 m
Number of riser tubes	66 per water panel
Riser tube dimensions	Sch. 160 1 inch (ID 0.815'', OD 1.315'')
Pitch-to-diameter ratio (calculated by OD)	4.0
Panel thickness	10 mm
Emissivity	0.8

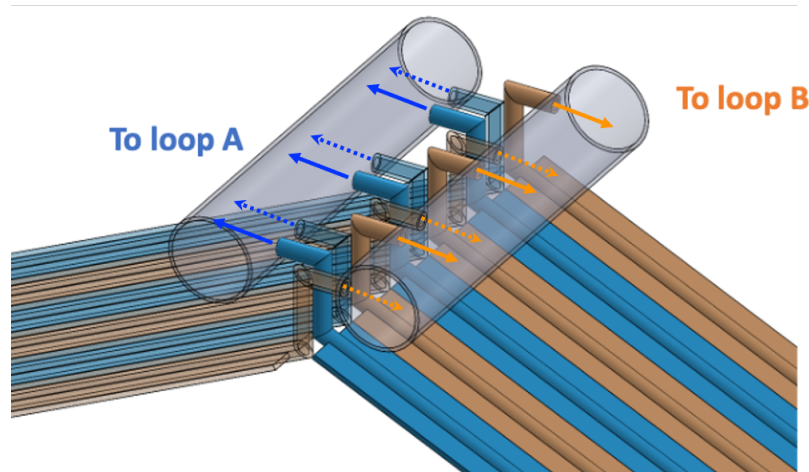


Figure 27 Connection between the upper plenum and the riser tubes

A group of 6 riser tubes are connected at each end to the bottom and the top collectors at the inlets and the outlets, respectively. To form two independently operating loops, the riser tubes in each loop have been alternately positioned to maintain a cooling capability on both sides of the RPV when one of loops fails. Figure 27 shows a potential configuration of connection details between the riser tubes and the upper collectors. Riser tube indicated in blue or orange color is arranged one after another and connected to the top collector. Each loop is isolated, but riser tubes thermally connected by the panels are located at each side of the RPV. This configuration enables to cool both sides of the RPV when one of the loops are not operating.

There are two water storage tanks in the RCCS circuit containing most of the water inventory. They can be vented to allow steam to escape as necessary by any passive means which maintains system pressure at atmospheric pressure. The sizing of the top tanks is determined based on the estimation of the system inventory to provide 7 days of decay heat removal until all coolant in the system is boiled off as described in Section 3.1.1. Water enters the tank 0.6 meters above the tank bottom and exits the tank through the downcomer. The top tank is positioned in the reactor building and its reference location remains above the RPV in the current design stage [19]. Final shape of the top tank might be updated to minimize reactor building radiation level from potential water activation. Currently, a single tank has been considered in each loop of the system, but each could be divided into multiple sections, if necessary, as the reactor building layout proceeded to optimization.

The RCCS tank cooling system controls the water temperature in the top tank maintaining a desired condition of the system, but its concept has not been established yet. Major features of the tank cooling system for the HC-HTGR RCCS could be adopted among previous efforts made on a generic HTGR RCCS but not limited to. For instance, SC-HTGR have considered a water-water heat exchanger within the RCCS water tank with connecting a circulating pump, valves, and air-cooled heat exchanger [3]. Water-based RCCS of Chinese HTR-10 adopted a cooler within an air chimney located outside the reactor cavity [20].

4.3 Operating conditions

The HC-HTGR RCCS can have distinct operating modes. During normal operation condition, all natural circulation loops are in operation. Therefore, there is a parasitic heat loss from the RPV which was estimated approximately 0.22 MW_t . The top tanks are cooled by the RCCS tank cooling system passively or actively depending on its design strategy. In this condition, subcooled single-phase natural circulation is expected. For accidents such as depressurized conduction cooldown (DCC) or pressurized conduction cooldown (PCC) events, the RCCS was designed both natural circulation loops are in operation but the heat load on the system might vary depending on the accident progression. The top tanks could be cooled by any means during accidents, but the design condition should consider their unavailability. In this case, water in the system will gradually heat up and ultimately reach saturation state which will have boiling. In long term cooling of this case, the system might loss a system inventory as a gradual boiled-off of the water in the system. In addition, since the conceptual RCCS for the HC-HTGR consists of two loops, there is a potential operation condition that only a single loop is in operation and the other is not operating. As the riser tubes connected to each loop is arranged evenly at both side of the RPV, single loop operation is still able to cool both side of the RPV, but a half of riser tubes are unable to transfer heat to one of the tanks.

5 Performance Evaluation of the HC-HTGR RCCS

Performance characteristics of the RCCS design would be addressed with consideration of a range of operation conditions such as two loop and single loop operation and various system heat loads. As the development of the HC-HTGR is currently in the early conceptual design phase, the reactor design sharing interfaces with RCCS will evolve over time being refined and optimized by a series of trade studies. For that reason, detailed analyses on RCCS performance will be pursued during later stages of the design process with final selections made regarding dimensions, materials, and more detailed elements of the reactor. Nevertheless, the design calculations performed in the conceptual design phase will confirm the RCCS performance being consistent with the passive safety approach under initially selected power level of the HC-HTGR. It also provides confidence in reducing risk of significant changes in the reactor design which would bring subsequent conceptual design studies in reactor designs sharing interfaces with the RCCS.

5.1 System-level performance of the HC-HTGR RCCS

5.1.1 RELAP5-3D model of the HC-HTGR RCCS

Figure 28 shows the nodalization diagram of the current RELAP5-3D model of the HC-HTGR RCCS. 6 riser tubes are modeled with vertical pipes, 1 inch Sch. 160 pipes (P301 to P306). The pipes feature bends of 115-degrees at the two initial and two final axial nodes as determined by their shapes. The top and the bottom collectors of the riser tubes are modeled as a series of branches, namely B201-B206 and B401-B406, respectively. The top water tank is modeled with three components, namely P550, P560, and B555, to represent the water tank volume below and above injection port and thermal mixing region, respectively. A series of connecting pipes is modeled with P600 to P620 from the top tank to the bottom collector and P510 from the top collector to the top tank. Each piping except the upper and lower collectors and the water tank are set to have a cross-sectional area scaled by 1/11 of actual dimensions as 6 are modeled among total of 66 riser tubes of each water panel, while setting actual diameters as hydraulic diameters for the scaled components.

The water panel is modeled with heat structures of 6 carbon steel cylindrical pipes and carbon steel flat plate panels. The pipes have convective boundary conditions for inner surfaces with water. The panels have adiabatic boundary conditions on right surfaces (opposite side facing the reactor building), which would be replaced with corresponding convective boundary conditions once reactor building configuration is available to reflect the actual condition. A half of the RPV was modeled as a carbon steel vertical flat plate with 7 axial nodes, where the inner RPV surface is set with the heat flux boundary condition. Conduction and radiation enclosures are employed to thermally connect all structures. As mentioned in Section 3.2.3, the water panel modeling approach to incorporate major heat transfer mechanisms of the RCCS has been adopted. In this approach, the inner surfaces of the pipes and right surfaces (outer surfaces) of the panels are set by a conduction enclosure to take account for the conduction heat transfer through the water panel and the outer surface of the RPV. Outer surfaces of the pipes and the left surfaces (inner surfaces facing the RPV) of the panels are set by a radiation enclosure. An emissivity for all participating surfaces are set as 0.8, and a series of view factors in actual configurations obtained from the STAR-CCM+ view factor calculation solver [10]. For the active cooling in the water tank and control the exit temperature of the water from the top tank, heat structure is connected to the top tank, which

consists of three pipe components. The tables of temperature and convective heat transfer coefficient was specified at the outer surface of it.

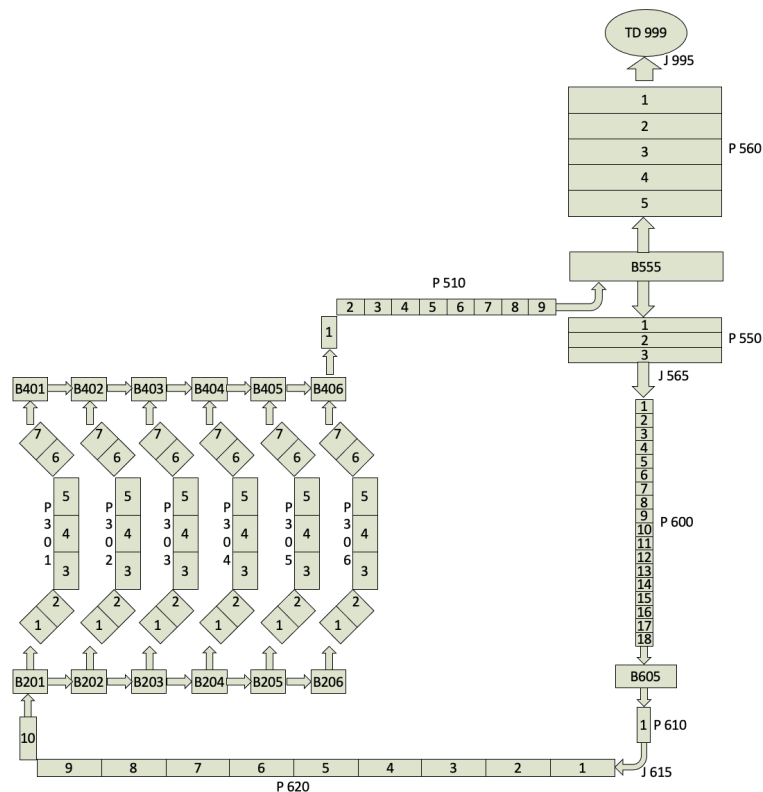


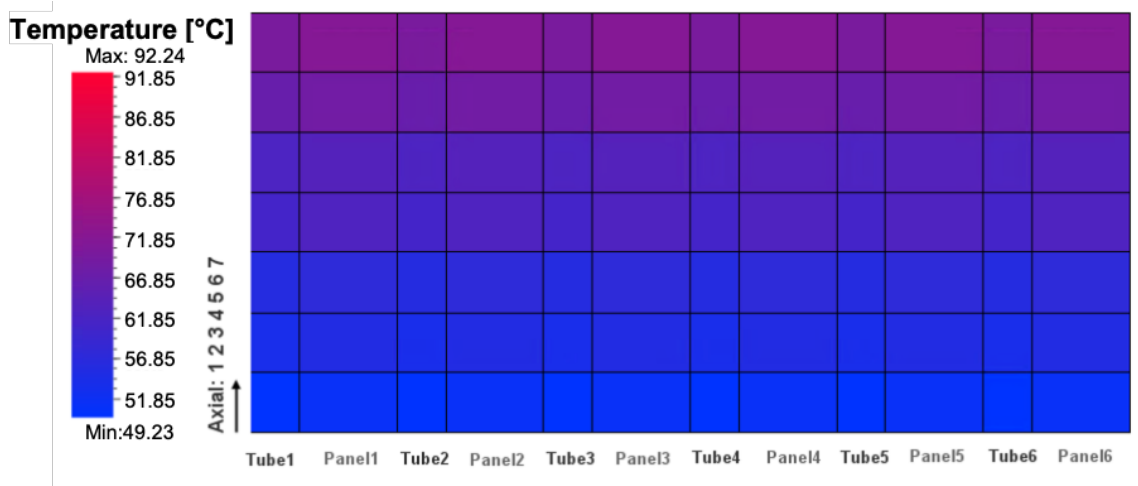
Figure 28 Nodalization diagram of the RELAP5-3D model used in design calculations

5.1.2 System performance by operating mode

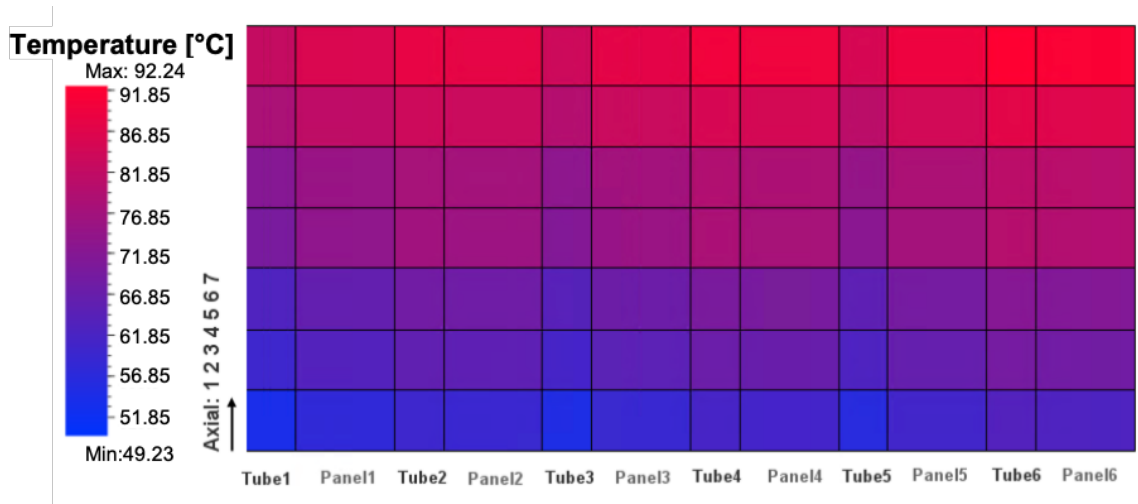
The configuration of the HC-HTGR RCCS allows for the cooling of both sides of the RPV, even when only a single loop is in operation. A single loop operation of the system would affect both panel conduction performance and natural circulation performance throughout the system. Compared to two-loops operation, the distance between working riser tubes will increase, therefore, the panel temperature and the heat load on individual riser tube will change significantly. Per current configuration of each loop, it is reasonable to assume that every alternate riser tube within the panel is included while the non-operational riser tubes in between remain empty during single loop operation of the RCCS. In the RELAP5 model, every other 3 riser tubes were connected to the loop (P301, P303, P305) and others (P302, P304, P306) were disconnected, while maintaining heat structures of the pipes and the interconnecting panels which allow conduction heat transfer between working riser tubes. Under the same design condition of two loop operation, a single loop operation was simulated with the RPV temperature of 420 °C and the controlled water exit temperature of 25 °C from the tank.

Figure 29 and Figure 30 show the water panel temperature distribution at the design condition by operation mode – two loops and single loop operation. For two loops operation, temperature differences between all 6 tubes and adjacent panels were fairly small of ~1.6 °C, with the maximum riser tube and panel temperatures being 69.98 °C and 71.61 °C, respectively. For single loop

operation, 3 working riser tubes (tube 1, tube 3, tube 5) had lower temperatures than 3 non-operating riser tubes (tube 2, tube 4, tube 6) as removing radiation heat from the RPV and conduction heat from adjacent panels by natural convection. Tube 6 and tube 5 had the maximum temperature of 92.23 °C and 85.46 °C respectively among all the non-operating and operating riser tubes. The maximum panel temperature was 91.66 °C at the panel 6. Mass flow rates in the operating riser tubes were 0.0895 kg/s, 0.0923 kg/s, and 0.0950 kg/s for tube 1, tube 3, and tube 5, respectively. The rightmost of the water panel had higher temperature from the flow direction of the lower and the upper collectors, where flow directions of both collectors in dividing and combining flow headers are modeled the same. The type of header is referred as a Z-manifold, where the channel flow rate generally increases in the direction of the intake stream [19]. Even if the water panel temperature shows asymmetric distribution, temperature gradient between non-operating rise tube and adjacent panel is up to ~4.8 °C, which is insignificant to structural integrity.



a) Two loops operation



b) Single loop operation (Only tube 1, 3, 5 are connected to the loop)

Figure 29 Comparison of the water panel temperature at the design condition by operation mode

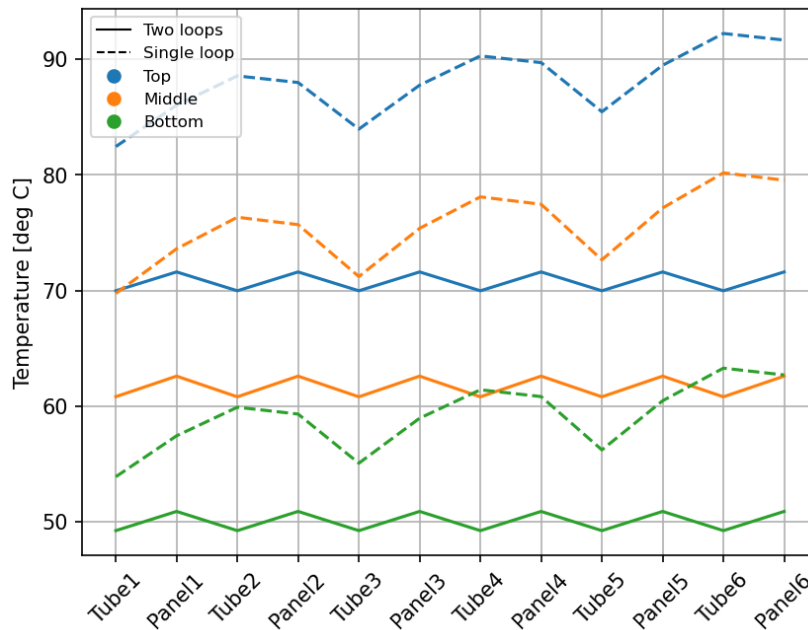


Figure 30 Temperature distribution of the water panel at the design condition by operation mode

Table 13 summarizes the comparison of RCCS performance of two loops operation and single loop operation at the design condition. The maximum water panel temperature increased by $\sim 20^\circ\text{C}$ in case of a single loop operation. Riser tube and panel temperatures rose, and total system mass flow rate decreased accordingly. However, the mass flow rate of each individual operating riser tube increased. It had a heat load on each individual riser tube doubled from not working half of the riser tubes. Overall, it showed a single loop operation had a similar level of thermal performance with the two loops operation.

Table 13 Performance of the RCCS at the design condition by operation mode

	Two loops	Single loop
System ΔT [$^\circ\text{C}$]	26.54	38.52
Maximum tube temperature [$^\circ\text{C}$]	69.98	92.23 (Non-operating) 85.46 (Operating)
Maximum panel temperature [$^\circ\text{C}$]	71.61	91.66
Average flow rate of individual riser tube [kg/s]	0.0676	0.0923
Average heat load on individual riser tube [kW]	7.50	14.86
System mass flow rate [kg/s]*	8.93	6.09
Total heat removal rate [MW]*	0.99	0.98

* Scaled by 22 to represent the entire system

5.1.3 System performance under various heat load conditions

System dynamics during transients is deemed important in the design process for various RCCS operating regimes expected. To cover expected RCCS operation conditions – beginning with single-phase natural circulation, progressing to two-phase natural circulation, and gradual boil-off of the coolant inventory of the system, the heat sink for the top water tank of the RCCS was assumed immediately unavailable at the initial stage of various heat load conditions. In this work, two heat load conditions have been considered for transient simulations in order to ensure the system operation maintains structural temperatures below the maximum allowable temperature with maintaining sufficient system inventory.

The most challenging heat removal event for a typical HTGR is a depressurized conduction cooldown (DCC). This type of accident is generally considered to be the defining accident for determining the reference case accident peak fuel temperature [22], therefore, it has been key consideration in design calculations to guide future design activities for design optimization of the RCCS. During the water-based natural convection shutdown heat removal test facility (NSTF) program, the prototype decay heat load to RCCS based on Framatome's 625 MW_t SC-HTGR was provided to the Argonne team [23,24]. Detailed conditions and assumptions made for DCC calculations to obtain the power profile during DCC for the SC-HTGR were business-sensitive. Taking the most conservative case (V.2) among available data, a specific power-time curve was created by post-processing. This involved normalizing the data using the heat load at time=0 s, which represents the parasitic heat loss during normal reactor operation and multiplying it by the parasitic heat loss of the current design of RCCS for the HC-HTGR under conditions of a constant RPV temperature of 220 °C (0.22 MW), which is expected during normal operation of the HC-HTGR.

Figure 31 shows the power-time curve considered for the HC-HTGR design calculation scaled from the estimated heat load during DCC by Framatome. The heat load to the RCCS initially decreased to 80 % of the parasitic heat loss within the first 7 hours, after which it began to rise to reach a peak heat load of 153 % of the parasitic heat loss and then reduced until 500 hours. The DCC heat load profile was imported to a heat flux-time table after converted for each axial node of the RPV and set for the left surface (inner surface) of the RPV. Initial conditions were obtained by running the RELAP model for 10⁵ sec with conditions of constant RPV temperature of 220 °C and the tank exit water temperature of 25 °C to ensure fully developed steady state. Then, the transient calculation was conducted for the heat load condition of hypothetical DCC event without heat sink for the water tank starting at 0 sec. The case was run using a restart model where one of the trips triggering the accident scenarios was set to true so convective heat transfer of the heat structure at the top tank was set to zero and the heat flux profile changed by the table provided.

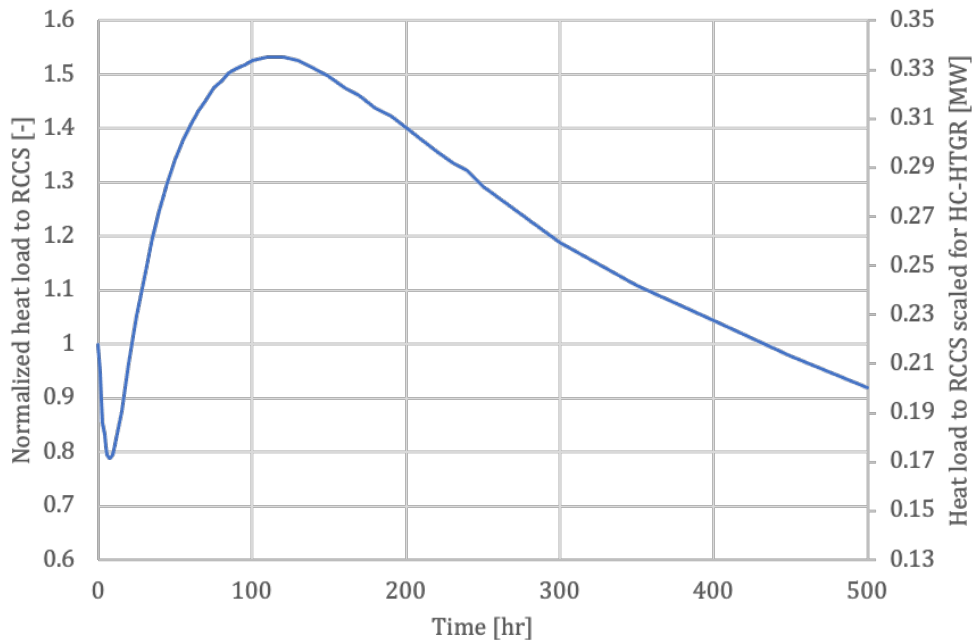
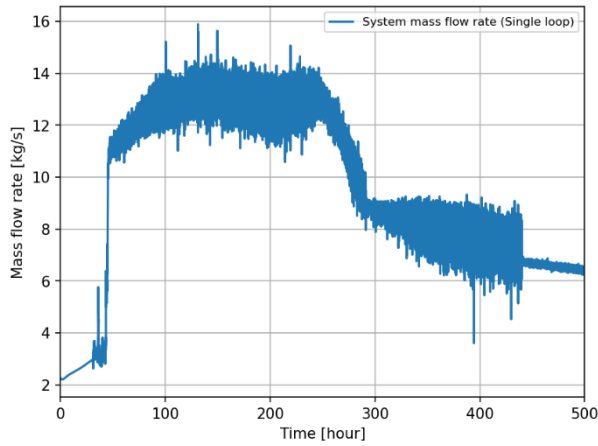
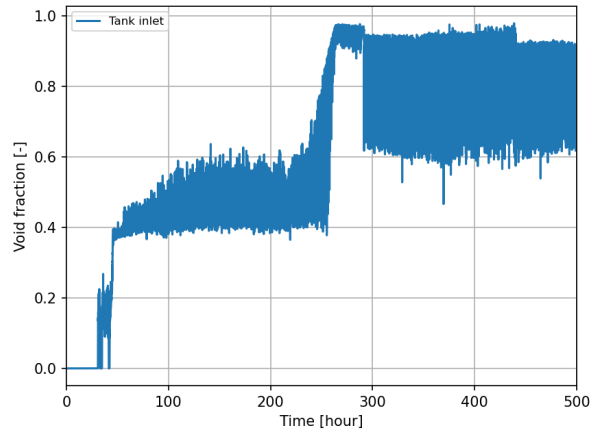


Figure 31 Heat load to RCCS during DCC (Scaled from Framatome's input) [17]

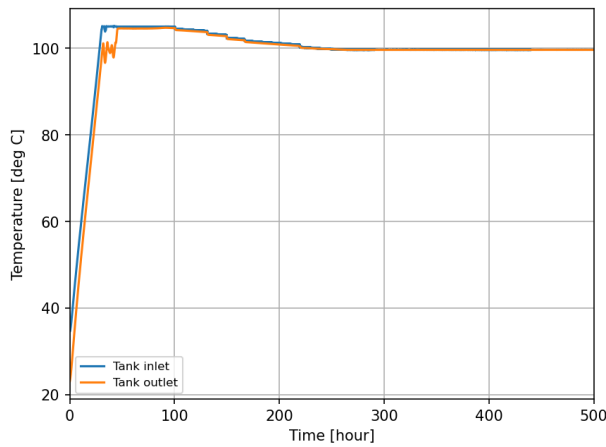
Figure 32 shows the transient behavior of the system during hypothetical DCC heat load condition. Starting with the single-phase natural circulation, the first overshoot of the mass flow rate occurred ~40 hours as flashing initiated at the horizontal returning pipe to water tank at the first node of the P510, and significant increase of the mass flow rate was followed. The coolant in the system kept heating up and quickly reached saturation temperatures corresponding to the tank inlet and outlet elevation. The tank inlet and outlet temperatures started to decrease after ~100 hours as the system inventory started to lose. Total coolant mass did not start to drop until 100 hours when steam coming from the riser tubes were initially condensed in the tank until the entire tank is saturated. It resulted in gradual decrease of system pressure accordingly. After ~250 hours, both tank inlet and outlet pressures were stabilized to the atmospheric pressure, as the top part of the tank (P560) was depleted, and their temperatures had saturation temperatures correspondingly. Overall, 67 % of the total water inventory was lost for 500 hours, and it took 370 hours to lose half of the system coolant under the hypothetical DCC heat load.



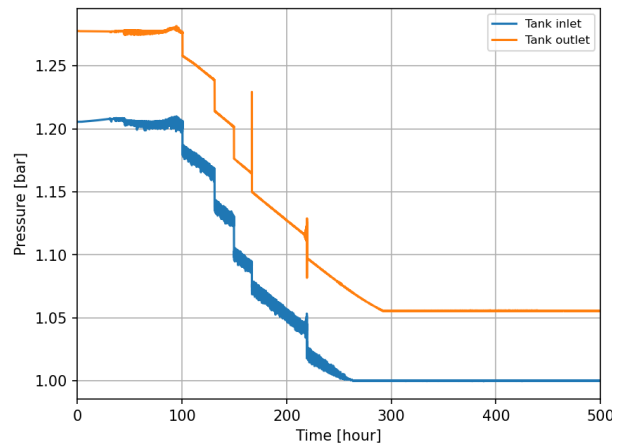
a) System mass flow rate (Scaled per loop)



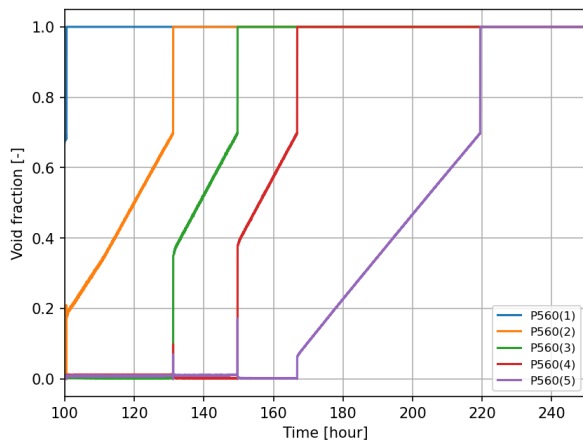
b) Void fraction at tank inlet (P510(9))



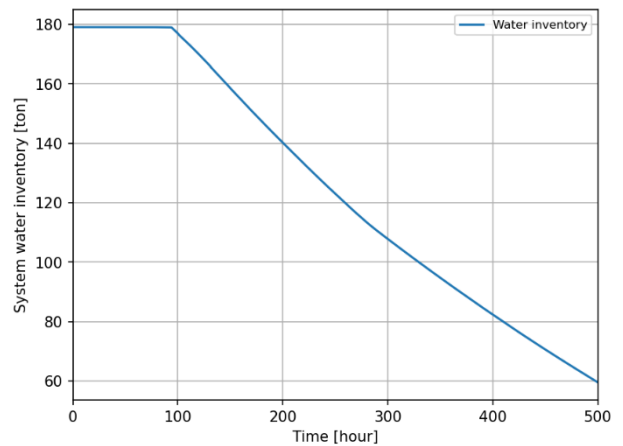
c) Tank inlet and outlet temperatures



d) Tank inlet and outlet pressures



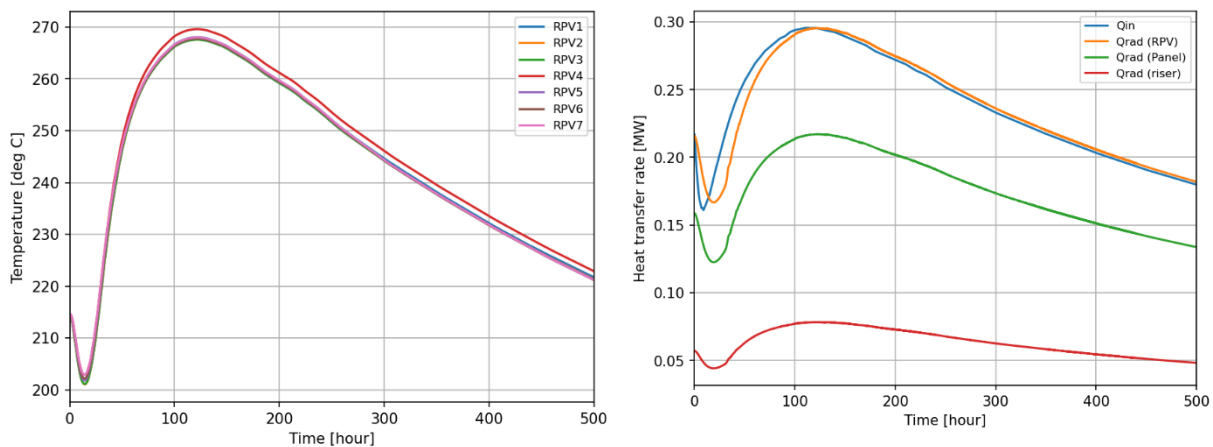
e) Void fraction of the tank (P560)



f) System coolant inventory

Figure 32 Transient behavior of RCCS for the HC-HTGR under the hypothetical DCC heat load

Figure 33 shows the changes of the RPV temperature and the radiative heat transfers over time under the hypothetical DCC heat load. The maximum RPV temperature was 269.6 °C at the center of the RPV in the axial direction after ~122 hours. Axial distribution of the RPV temperature was fairly even within ~ 2.0 °C. The RPV temperature overall followed the heat load exerted on the RPV, and it had its peak at the same time as that of peak RPV temperature, which was 12 hours later than the time of the maximum heat input at ~110 hours. The ratio of the radiative heat from the RPV to the panels and the riser tube outer surfaces maintains around 25 % and 75 % respectively for 500 hours, which aligns with the surface area ratio between the two. This confirms that the major affecting factor of the thermal performance is still the water panel area at the design condition, which have been updated accordingly.



a) RPV temperature

b) Heat flow

Figure 33 RCCS performance under the hypothetical DCC heat load

Subsequently, Boston Atomics provided the RPV heat flux profile to the Argonne team created as part of an in-core study of fuel performance and graphite properties estimated with the initial geometry of the HC-HTGR [24]. The conditions and assumptions made for creating the RPV heat flux profile are business-sensitive. As the core performance to the RCCS performance carries many uncertainties and imperfections until the design is finalized, the project team has been decided to use this only for a trial case for the RCCS analysis to avoid extrapolating analysis. Figure 34 shows the potential heat load to the RCCS of interests. The data only goes out to 100 hours, but they are sufficient to estimate a peak temperature when the vessel surface heat flux becomes steady. The new heat load profile was imported to a heat flux-time table and set for the left surface (inner surface) of the RPV. With the same initial conditions used for the hypothetical DCC simulations, the transient calculation was conducted under the new heat load without any heat sink available for the water tank. The calculation was run using a restart model where one of the trips triggering the accident scenarios was set to true so that convective heat transfer of the heat structure at the top tank was set to zero and the heat flux profile changed by the table provided.

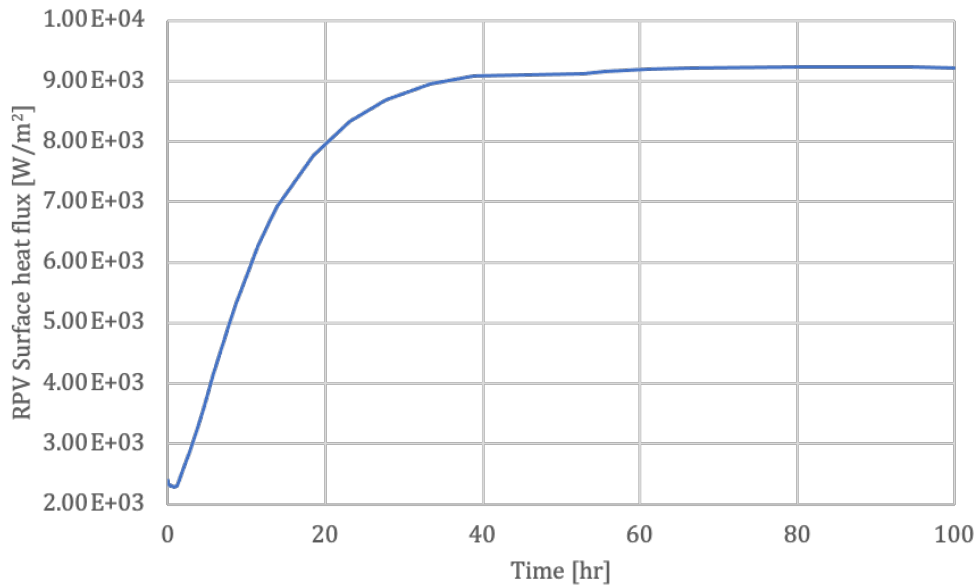
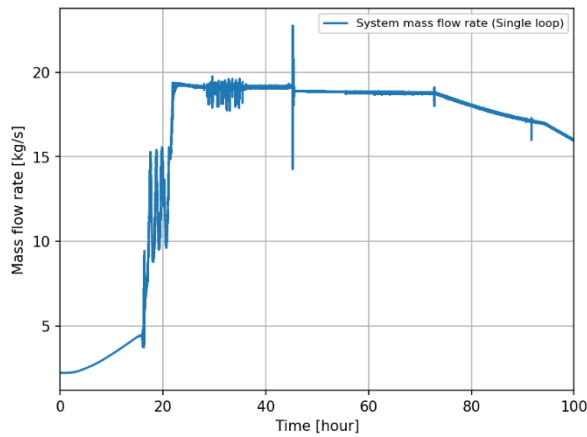


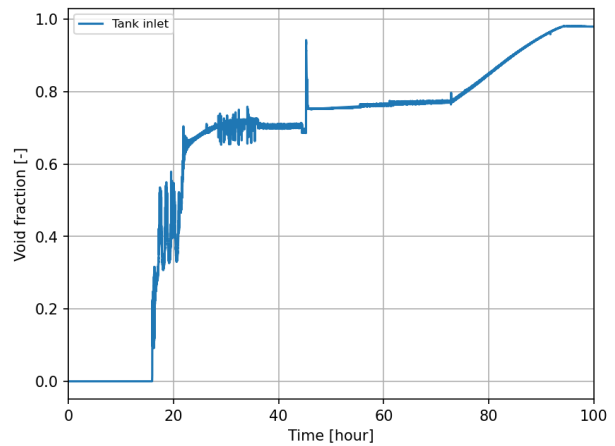
Figure 34 Heat load to RCCS bounding case provided by Boston Atomics – vessel average heat flux

Figure 35 shows the transient behavior of the system under the heat load Boston Atomics provided. Starting with the single-phase natural circulation, the first jump of the mass flow rate occurred ~ 17 hours as flashing initiated at the inlet of the horizontal returning pipe to water tank (P510) and significant increase followed. As the heat load increased continuously, the coolant in the system kept heating up and quickly reached saturation state. The second jump of the mass flow rate variation following significant reduction of the system pressure occurred at ~ 45 hours. It caused a sudden decrease of the top tank pressure and a quick depletion of coolant inventory of the top region of the tank (P560). This might be caused by an artificial effect due to modeling, which requires additional investigations, and it might be enhanced by turning on the level tracking option for the tank domain. Overall, 26 % of the total water inventory was lost for 100 hours under the heat load Boston Atomics provided for design calculations.

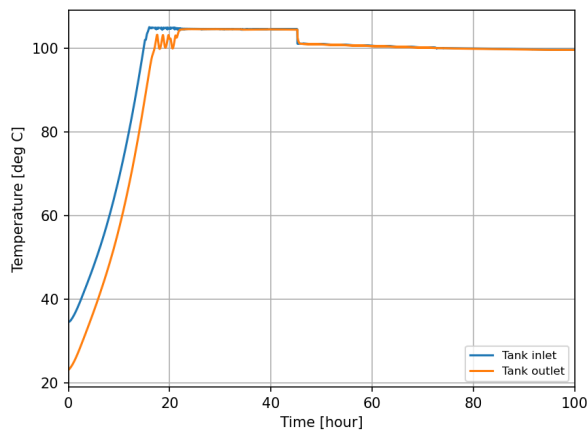
Figure 36 shows the changes of the RPV temperature and the heat flow over time under the heat load Boston Atomics provided. The maximum RPV temperature was $440.5\text{ }^{\circ}\text{C}$ at the center of the RPV in the axial direction at the end of the time period. Axial distribution of the RPV temperature was fairly consistent within $\sim 3.3\text{ }^{\circ}\text{C}$. The RPV temperature also followed the radiation heat transfer from the RPV, and it had its peak same with the time of peak RPV temperature with ~ 10 hours delay. Similar to the hypothetical DCC event results, the ratio of the radiative heat from the RPV to the panel and the riser tube outer surface maintains around 25 % and 75 % respectively.



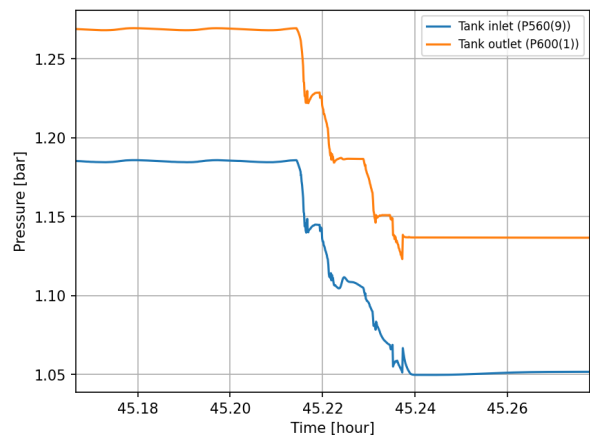
a) System mass flow rate (Scaled per a loop)



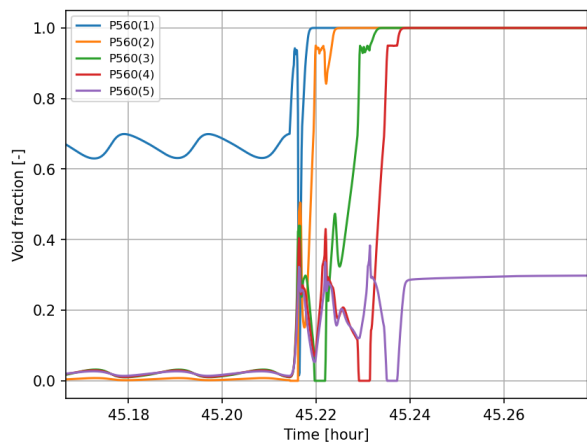
b) Void fraction at tank inlet (P510(9))



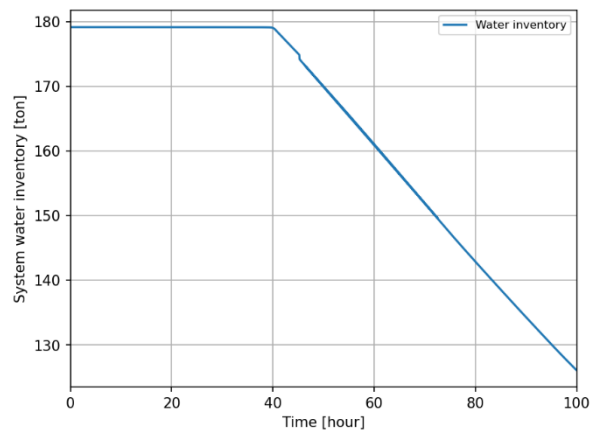
c) Tank inlet and outlet temperatures



d) Tank inlet and outlet pressures



e) Void fraction of the tank (P560)



f) System coolant inventory

Figure 35 Transient behavior of RCCS for the HC-HTGR under heat load provided by Boston Atomics

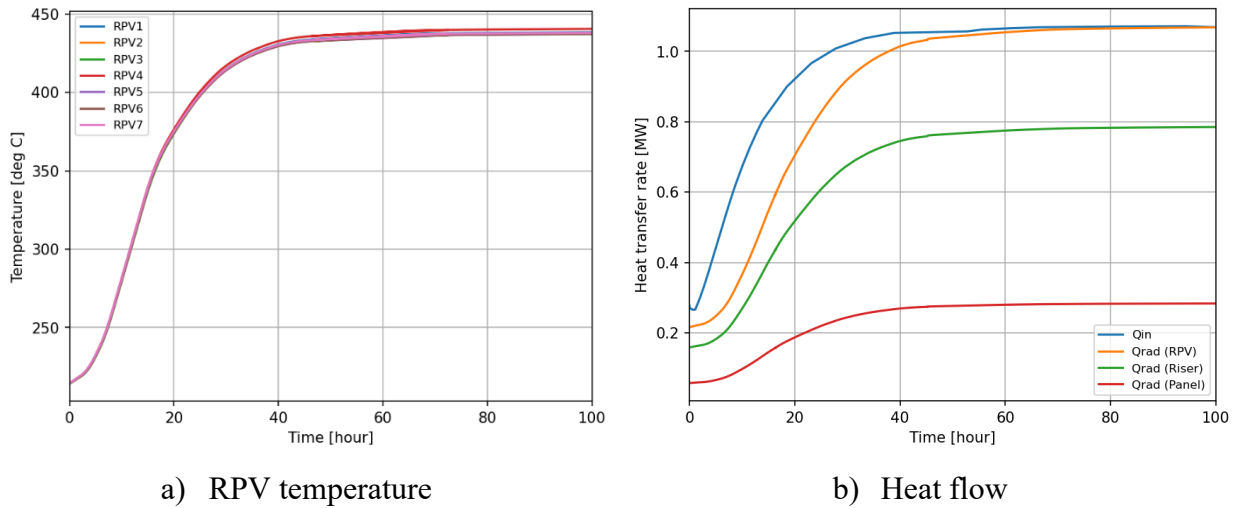


Figure 36 RCCS performance under heat load provided by Boston Atomics

Figure 37 shows the comparisons of the various heat load conditions used in this study along with a typical decay heat curve. The decay heat by time was approximated by using Wigner-Way formula assuming thermal power of 160 MW (P_0) with half year of the time elapsed before the shutdown in seconds (t_0) in equation (9). The heat load during hypothetical DCC approximated by Framatome’s SC-HTGR is way lower than decay heat curve for the first ~7 days (168 hours) but becomes close to the decay heat in long term. On the other hand, the heat load Boston Atomics provided is lower for the first 11-14 hours but becomes higher than the decay heat after then. It should be noted that the transient calculations with approximated heat load profiles would not be the actual conditions, which probably appears close to the heat load Boston Atomic provided for the first dozen hours, followed by a transition to a decay heat curve in the long term. The purpose of the transient calculations is to validate that the system design satisfies its design target. It was shown that the total system inventory would be sufficient to remove decay heat from the RPV for ~21 days (500 hours) without any active heat sink available for the RCCS, while maintaining low RPV temperatures based on the results of the hypothetical DCC simulation. The results under the Boston Atomics provided heat load condition also demonstrated that the maximum RPV temperature would maintain below the maximum allowable temperature by the RCCS operation. The current calculations are expected to demonstrate the overall system feasibility in the design process with certain transients addressed.

$$P_d = 0.0622P_0[t^{-0.2} - (t_0 + t)^{-0.2}] \quad (9)$$

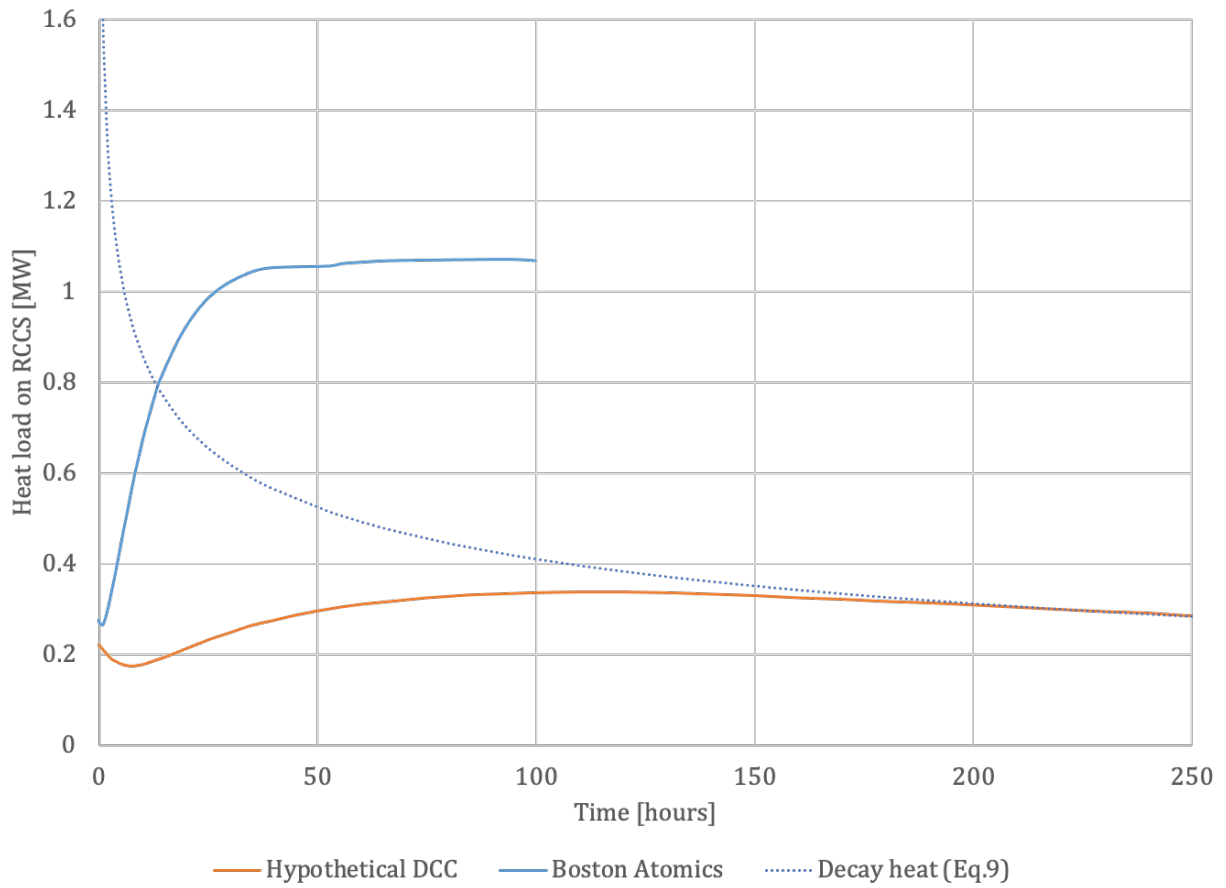


Figure 37 Comparison of various heat loads on RCCS with long term decay heat of HC-HTGR

6 Summary and Future Work

As part of the DOE-NE Advanced Reactor Demonstration Program's ARC-20 project, efforts have been made to derive the conceptual design of the RCCS which uses natural forces to provide safe and dependable ex-vessel cooling during emergencies by natural circulation for the HC-HTGR. A detailed concept of the RCCS has been identified, and the high-level system requirements have been developed for the HC-HTGR. Then, the design space focusing on the natural circulation loop portion of the RCCS has been investigated to optimize the system performance, and the initial baseline dimensions were initially derived based on the scoping calculations. Next, a component-level design analysis was conducted for the water panel to inform the material selection and to assess its conduction performance. A preliminary system-level performance analysis was performed for the 1/8th of the compartment of the initial baseline design of the RCCS using RELAP5-3D. To improve the system thermal performance, the RCCS design has been updated by exploring various design options by design parametric analyses. Based on the results, the conceptual design of the RCCS for the HC-HTGR has been derived.

The conceptual RCCS design is a water-cooled natural circulation system, which consists of the water panel embedding a series of riser tubes and a steel flat plate for the fins, the water tank, and connecting piping. It employs two independently operating loops to ensure system redundancy, where each of the RCCS loops consists of alternating channels with a single water panel. During normal operation, it is operated by a single-phase natural circulation with cooling the water tank, where the estimated parasitic heat loss from the RCCS operation is 0.22 MW_t. During accidents, it can be operated in a single-phase natural circulation if the water tank remains subcooled, where the estimated heat load on the RCCS is 0.99 MW_t at the RCCS design conditions defined in this study. If no heat sink is available for RCCS during accident conditions, the system can reach to the saturation after continuous heating up of the water and be operated in two-phase natural circulation to reject the decay heat. The system inventory was designed to assure up to 7 days until boiled off. During a single loop operation mode, the system still can provide sufficient cooling capability maintaining reasonable structural temperature. The system performance during accidents was estimated under various heat load conditions using RELAP5-3D. The results demonstrated the overall system feasibility in the design process with certain transients addressed.

The HC-HTGR RCCS will require additional design of subsystem(s) or optimization of the system components during the preliminary and final design phases. For instance, the system operational strategy might differ by the design of the RCCS water tank cooling system and its key component such as a heat exchanger. In addition, the heat load on the RCCS might vary depending on the reactor design and the accident progression, which was assumed at this design stage. This would be analyzed by the integrated RCCS and primary loop system analysis to simulate selective accident scenarios of interest. Other system interfaces with the RCCS such as shielding structural/seismic, primary system thermal hydraulics, etc. will be considered. Then, the performance assessment of the RCCS for the HC-HTGR would be revisited and optimized to finalize the system design.

References

1. W. R. Stewart, E. Velez-Lopez, R. Wiser, K. Shirvan, “Economic solution for low carbon process heat: A horizontal, compact high temperature gas reactor”, *Applied Energy*, 204, 117650, 2021.
2. Next Generation Nuclear Plant System Requirements Manual, Idaho National Laboratory, INL/EXT-07-12999, Rev. 2, 2009.
3. D. Lisowski, Q. Lv, B. Alexandreanu, Y. Chen, R. Hu, T. Sofu, “An Overview of Non-LWR Vessel Cooling Systems for Passive Decay Heat Removal,” ANL/NSE-21/3, May 2021.
4. Reactor cavity cooling system design description – Modular High-temperature Gas-cooled reactor, DOE-HTGR-87-068, 1987.
5. L. Lommers, F. Shahokhi, J. Hayer III, F. Southworth, “AREVA Modular Steam Cycle – High Temperature Gas-Cooled Reactor Development Progress”, *Proceedings of the HTR 2014*, October 2014.
6. American National Standard “Decay Heat Power in Light Water Reactors”, ANSI/ANS-5.1-2005.
7. R. E. Sund, “Afterheat calculations for the HTGR”, Gulf-GA-A12499, November 1973.
8. F. P. Incropera, D. P. DeWitt, T. L. Bergman, A. S. Lavine, “Fundamentals of Heat and Mass Transfer, 6th Edition”.
9. Q. Lv, A. Kraus, R. Hu, M. Bucknor, D. Lisowski, D. Nunez, “Progress Report on Computational Analyses of Water-Based NSTF,” ANL-ART-103, August 2017.
10. Siemens, Simsenter STAR-CCM+, v.2202.1 User Guide, 2020.
11. E. F. C. Somerscales and M. Kassemi, “Fouling due to corrosion products formed on a heat transfer surface,” *Journal of Heat Transfer*, Vol 109(1), pp. 267-271 (1987).
12. M. M. Awad, “Fouling of heat transfer surface,” In A. Belmiloudi (Ed.), *Heat Transfer – Theoretical Analysis, Experimental Investigations and Industrial Systems*, InTech. doi:10.5772/1756
13. J. Nesta and C. A. Bennett, “Fouling mitigation by design,” *Proceedings of 6th International Conference on Heat Exchanger Fouling and Cleaning – Challenges and Opportunities*, Kloster Irsee, Germany, June 5-10, 2005.
14. I. B. Butler, M. A. A. Schoonen, D. T. Rickard, “Removal of dissolved oxygen from water: A comparison of four common techniques,” *Talanta*, Vol. 41(2), pp. 211-215 (1994).
15. The RELAP5-3D Code Development Team, RELAP5-3D Code Manual Volume I: Code Structure, System Models, and Solution Methods, INL/MIS-15-36723, Rev. 4.3, October 2015.
16. R. Vaghetto, Y. Hassan, “Modeling the thermal-hydraulic behavior of the reactor cavity cooling system using RELAP5-3D”, *Annals of Nuclear Energy*, Vol. 73, pp. 75-83, 2014.
17. Y. Jeong, D. Lisowski, Q. Lv, R. Hu, “Preliminary Design of Reactor Cavity Cooling System for a Horizontal Compact HTGR”, ANL/NSE-22/72, September 2022.
18. Framatome Inc., “Reactor cavity cooling system (RCCS) Heat load during SC-HTGR depressurized conduction cooldown (DCC) events,” Document no. 12-9346789-000 (2022).
19. W. R. Stewart, Private communications, April 25th, 2023.
20. T. D. Roberto, C. M. F. Lapa, A. C. M. Alvim, “Scaling Analysis of Reactor Cavity Cooling System in HTR,” *Nuclear Technology*, Vol. 206, pp. 527-543 (2020).

21. J. M. Hassan, W. S. Mohammed, T. A. Mohamed, W. H. Alawee, “Review on Single-Phase Fluid Flow Distribution in Manifold,” International Journal of Science and Research, 3(1), pp.325-330, 2014.
22. S. J. Ball, “Overview of Modular HTGR Safety Characterization and Postulated Accident Behavior Licensing Strategy,” ORNL/TM-2014/187, May 2014.
23. Q. Lv, M. Jasica, R. Hu, Z. Ooi, M. Farmer, D. Lisowski, “Report on Year-4 Water NSTR Matrix Testing,” ANL-ART-256, September 2022.
24. W. R. Stewart, Private communications, August 23rd, 2023.

Acknowledgement

This work is funded by U.S. Department of Energy Office of Nuclear Energy’s Advanced Reactor Concepts-20 (ARC-20) program.



Nuclear Science and Engineering Division

Argonne National Laboratory
9700 South Cass Avenue, Bldg. 208
Argonne, IL 60439

www.anl.gov



**U.S. DEPARTMENT OF
ENERGY**

Argonne National Laboratory is a U.S. Department of Energy
laboratory managed by UChicago Argonne, LLC